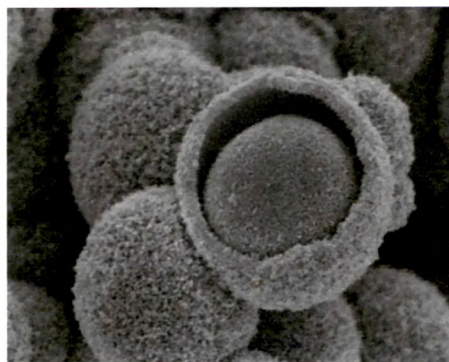


Chapter 1

Preparation & Characterization



Recently nanoparticulate drug delivery systems are gaining interest due to their potential to improve current drug therapies because of their ability to overcome multiple biological barriers, ability to deliver drugs in the optimum dosage range, resulting in increased therapeutic efficacy of the drug, reduced side effects, and improved patient compliance (Alexis et al., 2008). Amongst the nanoparticle delivery systems, polymeric nanoparticles (NPs) have shown promising properties for targeted drug delivery and for sustained action. These are colloidal systems that range in size typically from 10-1000 nm in diameter and are formulated from a biodegradable polymer in which the therapeutic agent is entrapped, adsorbed or chemically coupled onto the polymer matrix (Labhasetwar, 1997).

An array of polymers and techniques for preparation of nanoparticles are available and hence depending on the physicochemical characteristics of a drug, it is possible to choose the best method of preparation and the best polymer to achieve an efficient entrapment of the drug along with required particle size. In last decade, there is an increased interest in developing nanoparticles from biodegradable polymers since they offer a suitable means of delivering small molecular weight drugs, proteins or genes by either localized or targeted delivery to the tissue of interest in addition to their low toxicity profiles (Gan, 2010). Although a number of different polymers have been investigated for formulating biodegradable nanoparticles, poly- ϵ -caprolactone (PCL), poly (lactide-co-glycolide) (PLGA) and poly lactic acid (PLA) are FDA approved biocompatible and biodegradable polymers. In this regard, PLGA nanoparticles with entrapped therapeutics are of special interest for drug delivery owing to

their biocompatibility, biodegradability and ability to sustain therapeutic drug levels for prolonged period of time. The polymeric matrix prevents the rapid degradation of drug, and also allows precise control over the release kinetics of the drug from NPs. Moreover, the duration and level of drug released from the NPs can be easily modulated by altering formulation parameters such as drug: polymer ratio, or polymer molecular weight and composition (Vasir and Labhasetwar, 2007).

Various methods used for the preparation of PLGA nanoparticles include emulsification/solvent evaporation, emulsification/solvent diffusion, solvent displacement/diffusion (nanoprecipitation), and salting out using preformed synthetic polymers. In the present study, nanoprecipitation method was utilized for preparation of nanoparticles as this method leads to formation of submicron particles with narrow size distribution (Fessi et al., 1989). Further, emulsion-solvent evaporation was also utilized to improve the drug entrapment efficiency (Sahoo et al., 2002, Scholes et al., 1993).

The various tunable parameters of nanoparticle which affect the interaction of nanoparticles with biological barriers include composition, size, core properties, surface modifications (pegylation and surface charge), and finally, targeting ligand functionalization. All these factors have been shown to substantially affect the biodistribution and blood circulation half-life of circulating nanoparticles by reducing the level of nonspecific uptake, delaying opsonization and increasing the extent of tissue specific accumulation.

Surface functionalization can be utilized to increase residence time in the blood, reduce nonspecific distribution and in some cases, target tissues or specific cell surface antigens with a targeting ligand (e.g. peptide, aptamer, antibody/antibody fragment, small molecule). Among the various peptides

finding use in biomedical applications, transferrin (Tf) is also used as a ligand for targeting of drugs. The primary function of transferrin, a glycoprotein found abundantly in the blood, is to transport iron from the blood to cells through the transferrin receptors (TfR) (Qian and Tang, 1995; Andrews, 2000). TfR are over expressed in certain body tissues such as liver, epidermis, intestinal epithelium, vascular endothelium of the brain capillary, and certain populations of blood cells in the bone marrow (Li and Qian, 2002; Li et al., 2002). The approach of Tf conjugation has been specifically investigated for the delivery of therapeutic agents to the brain because Tf ligand can facilitate the transcytosis of the conjugated drug carrier systems across the blood-brain barrier (BBB) (Bickel et al., 2001; Pardridge, 2002). Another motivation for using Tf as a ligand is its potential to overcome drug resistance due to the membrane-associated drug resistant (MDR) proteins such as P-glycoprotein (P-gp) and Breast Cancer Resistant Protein (BCRP).

Hence, in the present study polymer (PLGA) concentration, loading amount of drug, concentration of tween-80, Polyvinyl alcohol (PVA) concentration, polaxamer (PLX) concentration, volume of organic phase, stirring speed and stirring time were optimized in order to obtain nanoparticles having minimum particle size with maximum drug entrapment efficiency.

Surface modification of PLGA nanoparticles was carried out by conjugating transferrin as a ligand. The ligand binds specifically to the receptors on the plasma membrane of the target tissue which leads to the internalization of plasma membrane receptors along with the delivery system i.e. NPs.

It is important to mention that characterization is a very important step in the formulation development. The *in-vitro* tests are carried out to predict the *in-vivo* behavior of the formulation. For its optimum performance *in-vivo*, the

formulation should possess specific characteristics. *In-vitro* tests are very helpful in the comparison of the formulations having different compositions and choosing the one that is best for further *in-vivo* studies. For intra-venous drug administration, the particle size of the nanoparticles should be below 200 nm so that the particles are not taken up by the reticuloendothelial system (RES). The % entrapment efficiency of the carrier should be high so that the amount of the formulation that has to be injected is less with minimum wastage of the drug. The drug should be released in a controlled manner so that the target site is not exposed to a significant amount of drug at a time and the drug is slowly released to give a sustained effect. Thus keeping these characteristics in mind, the nanoparticles were characterized for particle size, polydispersity index, zeta potential, drug entrapment efficiency, *in vitro* drug release, morphology, thermal characteristics and physicochemical properties. The various techniques utilized included -

- Photon correlation spectroscopy (PCS) based on the diffraction light scattering (DLS) for particle size and particle size distribution.
- Surface charge by measurement of zeta potential, morphology by transmission electron microscopy (TEM).
- Fourier Transform Infra Red Spectroscopy (FTIR) to confirm ligand conjugation to the surface of nanoparticles and also for drug identification.
- The entrapment efficiency was determined by estimation of drug in nanoparticles by spectrophotometry.
- *In vitro* release of drug from the nanoparticles was determined by dialysis tube diffusion technique.
- Thermogravimetric Analysis (TGA) was used to analyze thermal characteristics of the formulations.
- X-Ray Diffraction (XRD) was used for determining physical characteristics i.e. the crystalline or amorphous nature of the formulations.

5.1 PREPARATION OF PLGA NANOPARTICLES

5.1.1 Nanoprecipitation Method

PLGA nanoparticles were prepared by nanoprecipitation method reported by Fessi et al. (1989), with slight modifications. The basic process parameters like rate of addition of organic phase, stirring speed, volume of aqueous phase and stirring time were standardized before proceeding for the optimization of the formulation variables. These process parameters were standardized using qualitative examination of nanoparticle dispersion of placebo batches i.e. NPs prepared without drug. The rate of addition of organic phase was kept at 0.5 mL/min throughout the optimization process.

Pioglitazone loaded PLGA nanoparticles (PIO-NPN) were prepared by nanoprecipitation technique, on the basis of preliminary experimentation. The critical formulation parameters investigated included polymer concentration, amount of loading drug, surfactant (Tween-80) concentration, stabilizer (PVA) concentration and volume of organic phase for polymer as well as for drug.

Briefly, polymer (corresponding to 0.1 - 0.4% w/v of aqueous phase) was dissolved in acetonitrile (ACN) (3 - 6 ml) and drug (PIO) (1 - 4mg) was dissolved in methanol (MeOH) (1 - 4 mL). Drug solution was mixed with the polymer solution and this mixture was injected into 10 mL of aqueous phase containing 0.25 - 1.0% w/v PVA and 0 - 0.002 % w/v Tween 80 while kept for continuous stirring on a magnetic stirrer (Spectralab Whirlmatic Mega Stirrer, India).

With the diffusion of solvent into the aqueous phase, the polymer precipitates out while entrapping PIO leading to formation of pioglitazone loaded nanoparticles (PIO-NPN). The resulting nanoparticles dispersion was further stirred for 5 hrs to completely evaporate the organic phase. The colloidal dispersion so formed was centrifuged (Sigma 3K30 refrigerated high speed

laboratory centrifuge; Sigma Instruments, Osterode, Germany) at 3000 rpm for 15 min at 18°C to remove untrapped drug (which generally precipitates out) excluding untrapped solubilized drug. The supernatant was separated from the pellet of the precipitated drug and again centrifuged at 11,000 rpm for 15 min at 2°C to separate untrapped solubilized drug and hence it will not interfere with the estimation of entrapped drug. The pellet so formed was washed thrice with distilled water to remove excess PVA and was suspended in PBS (pH 7.4) by sonication and vortexing and proceeded for further characterization.

ROS loaded nanoparticles (ROS-NPN) were also prepared using the similar procedure and parameters as with PIO-NPN.

5.1.1.2 Optimization

Nanoparticulate formulations were optimized for formulation variables like concentration of polymer (PLGA), drug amount (PIO/ROS-B), concentration of surfactant (Tween 80), concentration of stabilizer (PVA), and volume of organic phase. Concentration of polymer was varied from 0.1 to 0.4% w/v of aqueous phase while keeping the other variables constant. Subsequently other variables i.e. loading drug amount (1 - 4 mg), Tween-80 concentration (0 - 0.002%), PVA concentration (0.25 - 1.0%) and further organic phase for polymer (3 - 6ml) and organic phase for drug (1 - 4 ml) were studied (Table 5.1 & 5.2 and Fig. 5.1 - 5.12).

Table 5.1: Optimization of formulation parameters for Pioglitazone formulations prepared by nanoprecipitation method

Formulation n code	PLGA Conc. (%w/v)	Amount of Drug (mg)	Tween 80 Conc. (% w/v)	PVA Conc. (% w/v)	Organic Phase for Polymer (mL)	Organic Phase for Drug (mL)	Average Particle Size (nm)	PDI	zeta Potential (mV)	%EE
PIO-NPN1	0.1	2.0	0.001	0.25	5.0	2.0	135.5±7	0.365	-7.8	12.9±1.2
PIO-NPN2	0.2	2.0	0.001	0.25	5.0	2.0	145.4±9	0.258	-11.0	19.9±1.1
PIO-NPN3	0.3	2.0	0.001	0.25	5.0	2.0	161.1±4	0.180	-18.3	23.1±2.1
PIO-NPN4	0.4	2.0	0.001	0.25	5.0	2.0	175.9±8	0.153	-22.8	29.5±1.3
PIO-NPN5	0.2	1.0	0.001	0.25	5.0	2.0	123.5±8	0.157	-5.83	19.7±1.3
PIO-NPN6	0.2	2.0	0.001	0.25	5.0	2.0	138.4±6	0.240	-5.20	24.1±1.4
PIO-NPN7	0.2	3.0	0.001	0.25	5.0	2.0	164.7±7	0.200	-5.43	16.9±1.0
PIO-NPN8	0.2	4.0	0.001	0.25	5.0	2.0	-	-	-	-
PIO-NPN9	0.2	2.0	0	0.25	5.0	2.0	-	-	-	-
PIO-NPN10	0.2	2.0	0.0005	0.25	5.0	2.0	269±18	0.382	-18.8	17.1±1.4
PIO-NPN11	0.2	2.0	0.001	0.25	5.0	2.0	145.9±5	0.148	-14.6	25.3±1.2
PIO-NPN12	0.2	2.0	0.002	0.25	5.0	2.0	114.8±6	0.214	-11.6	10.3±1.3
PIO-NPN13	0.2	2.0	0.001	0.25	5.0	2.0	135.6±7	0.210	-5.51	24.8±1.0
PIO-NPN14	0.2	2.0	0.001	0.50	5.0	2.0	147.3±6	0.348	-3.86	26.8±0.9
PIO-NPN15	0.2	2.0	0.001	0.75	5.0	2.0	180.4±8	0.305	-7.89	27.1±0.6
PIO-NPN16	0.2	2.0	0.001	1.0	5.0	2.0	240.7±6	0.275	-9.41	26.1±1.5
PIO-NPN17	0.2	2.0	0.001	0.25	3.0	2.0	152.7±9	0.146	-13.8	27.1±1.1
PIO-NPN18	0.2	2.0	0.001	0.25	4.0	2.0	135.9±4	0.203	-14.11	24.8±1.3
PIO-NPN19	0.2	2.0	0.001	0.25	5.0	2.0	124.9±6	0.463	-8.61	23.5±0.5
PIO-NPN20	0.2	2.0	0.001	0.25	6.0	2.0	112.6±7	0.385	-7.22	15.4±1.3
PIO-NPN21	0.2	2.0	0.001	0.25	5.0	1.0	331±25	0.394	-18.11	4.8±1.2
PIO-NPN22	0.2	2.0	0.001	0.25	5.0	2.0	139.2±4	0.221	-9.86	26.7±1.4
PIO-NPN23	0.2	2.0	0.001	0.25	5.0	3.0	190.2±8	0.120	-6.12	23.9±0.8
PIO-NPN24	0.2	2.0	0.001	0.25	5.0	4.0	-	-	-	-

-- indicates no nanoparticle formation; Average particle size, PDI, Zeta Potential and %EE values are average of 3 values ; p<0.05

Table 5.2: Optimization of formulation parameters for Rosiglitazone formulations prepared by nanoprecipitation method

Formulation n code	PLGA Conc. (%w/v)	Amount of Drug (mg)	Tween80 Conc. (%w/v)	PVA Conc. (%w/v)	Organic Phase for Polymer (mL)	Organic Phase for Drug (mL)	Average Particle Size (nm)	PDI	Zeta Potential (mV)	%EE
ROS-NPN1	0.1	2.0	0.001	0.25	5.0	2.0	127.3±8	0.262	-9.23	9.7±1.0
ROS-NPN2	0.2	2.0	0.001	0.25	5.0	2.0	129.4±6	0.228	-13.22	26.5±0.9
ROS-NPN3	0.3	2.0	0.001	0.25	5.0	2.0	139.3±4	0.179	-16.10	24.6±1.3
ROS-NPN4	0.4	2.0	0.001	0.25	5.0	2.0	158.2±8	0.145	18.98	27.8±0.8
ROS-NPN5	0.2	1.0	0.001	0.25	5.0	2.0	120.2±6	0.317	-15.31	15.7±1.0
ROS-NPN6	0.2	2.0	0.001	0.25	5.0	2.0	136.7±4	0.293	-12.43	27.5±0.8
ROS-NPN7	0.2	3.0	0.001	0.25	5.0	2.0	144.6±5	0.190	-8.32	18.2±0.9
ROS-NPN8	0.2	4.0	0.001	0.25	5.0	2.0	142.3±8	0.198	-5.37	14.3±1.2
ROS-NPN9	0.2	2.0	0	0.25	5.0	2.0	-	-	-	-
ROS-NPN10	0.2	2.0	0.0005	0.25	5.0	2.0	229.1±9	0.282	-15.52	19.1±1.1
ROS-NPN11	0.2	2.0	0.001	0.25	5.0	2.0	119.9±4	0.152	-12.20	28.8±1.0
ROS-NPN12	0.2	2.0	0.002	0.25	5.0	2.0	103.6±6	0.221	-8.22	8.1±0.8
ROS-NPN13	0.2	2.0	0.001	0.25	5.0	2.0	112.2±7	0.169	-12.1	26.3±1.1
ROS-NPN14	0.2	2.0	0.001	0.50	5.0	2.0	135.4±4	0.180	-18.2	28.6±0.6
ROS-NPN15	0.2	2.0	0.001	0.75	5.0	2.0	148.4±4	0.153	-23.9	29.1±0.9
ROS-NPN16	0.2	2.0	0.001	1.0	5.0	2.0	157.6±6	0.127	-30.1	28.3±1.1
ROS-NPN17	0.2	2.0	0.001	0.25	3.0	2.0	165.2±9	0.132	-5.8	28.1±0.9
ROS-NPN18	0.2	2.0	0.001	0.25	4.0	2.0	159.8±12	0.211	-9.22	26.2±1.1
ROS-NPN19	0.2	2.0	0.001	0.25	5.0	2.0	124.8±5	0.281	-11.26	27.6±0.9
ROS-NPN20	0.2	2.0	0.001	0.25	6.0	2.0	120.2±10	0.295	-14.68	13.7±1.4
ROS-NPN21	0.2	2.0	0.001	0.25	5.0	1.0	-	-	-	-
ROS-NPN22	0.2	2.0	0.001	0.25	5.0	2.0	125.7±6	0.223	-13.12	29.2±0.9
ROS-NPN23	0.2	2.0	0.001	0.25	5.0	3.0	149.2±9	0.302	-10.78	25.1±0.6
ROS-NPN24	0.2	2.0	0.001	0.25	5.0	4.0	-	-	-	-

'-' indicates no nanoparticle formation; Average particle size, PDI, Zeta Potential and %EE values are average of 3 values ; p<0.05

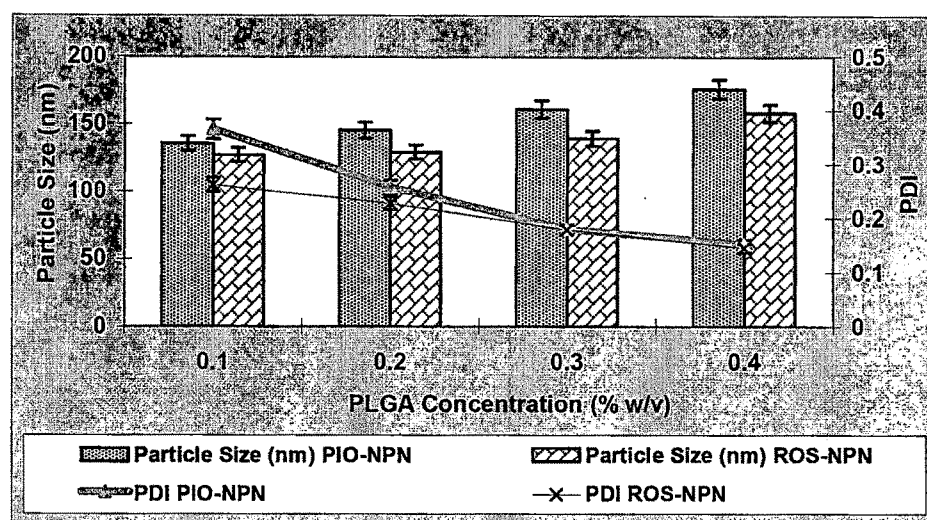


Figure 5.1 : Optimization of PLGA concentration with respect to particle size and PDI

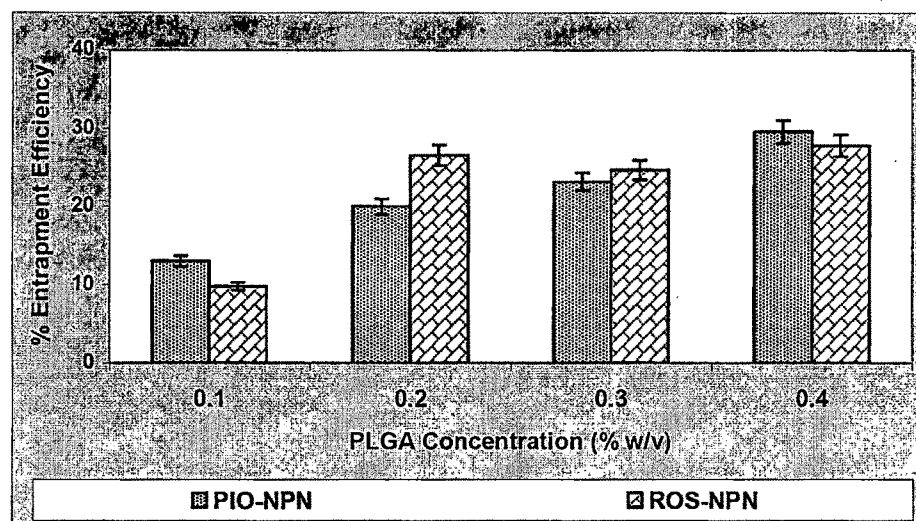


Figure 5.2 : Optimization of PLGA concentration with respect to entrapment efficiency

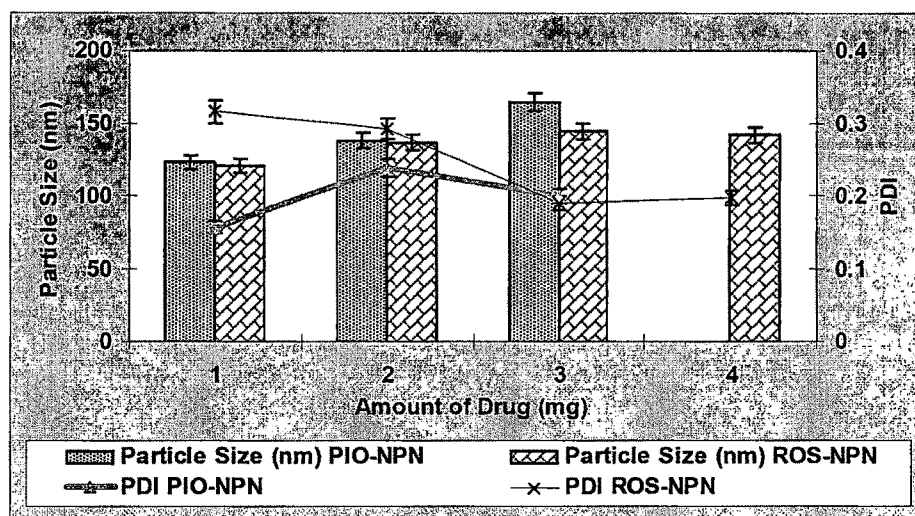


Figure 5.3: Optimization of loading amount of drug with respect to particle size and PDI

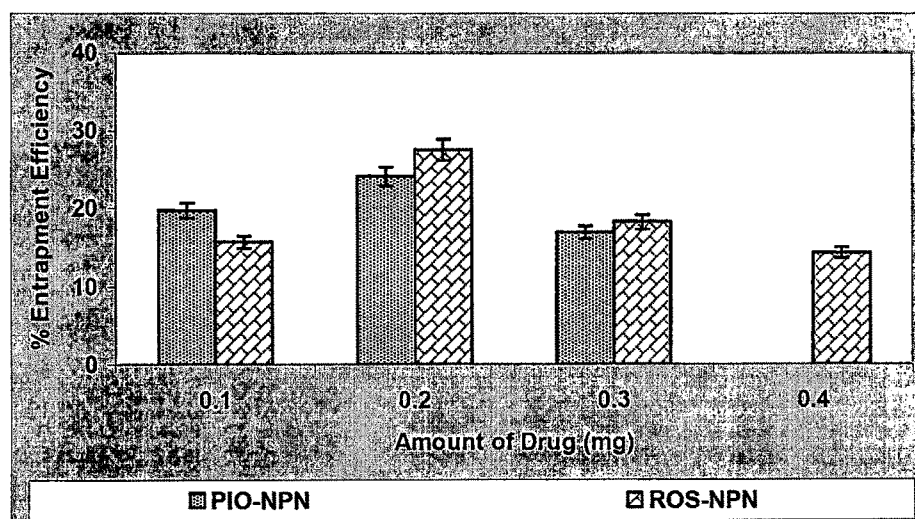


Figure 5.4: Optimization of the amount of drug with respect to entrapment efficiency

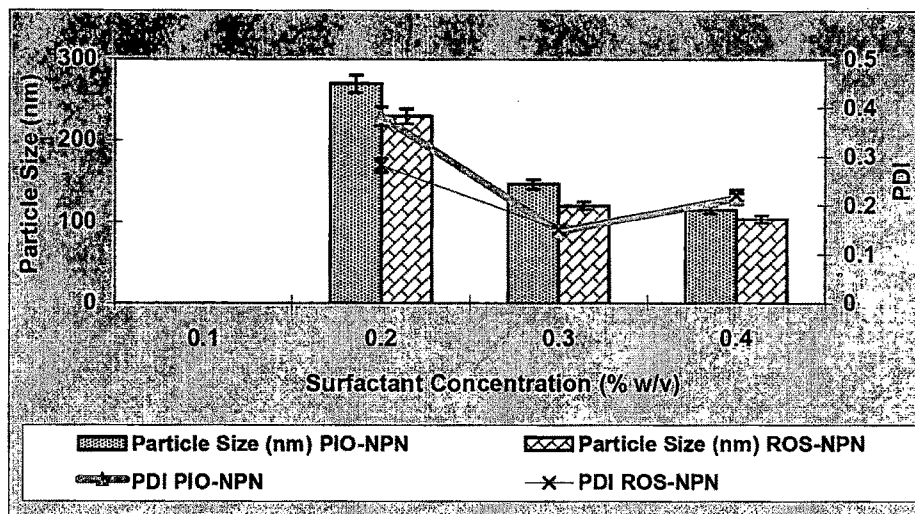


Figure 5.5: Optimization of surfactant concentration with respect to particle size and PDI

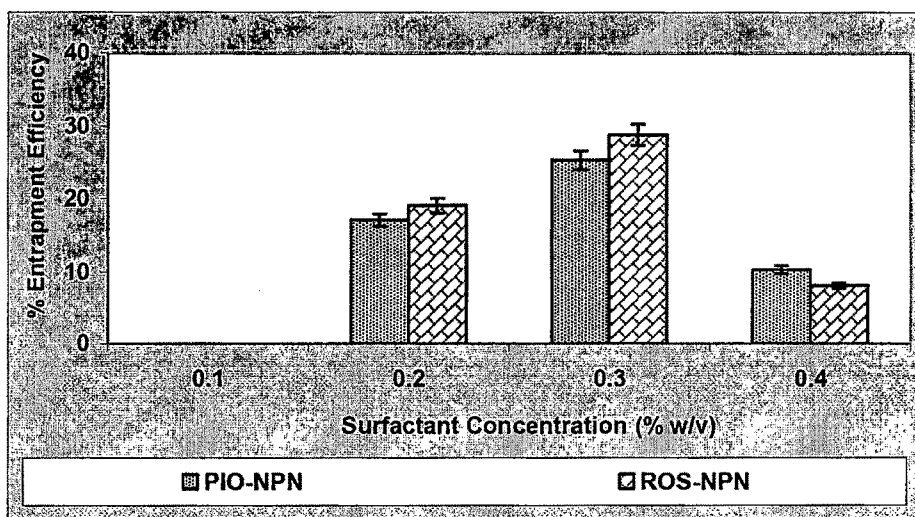


Figure 5.6: Optimization of surfactant concentration with respect to entrapment efficiency

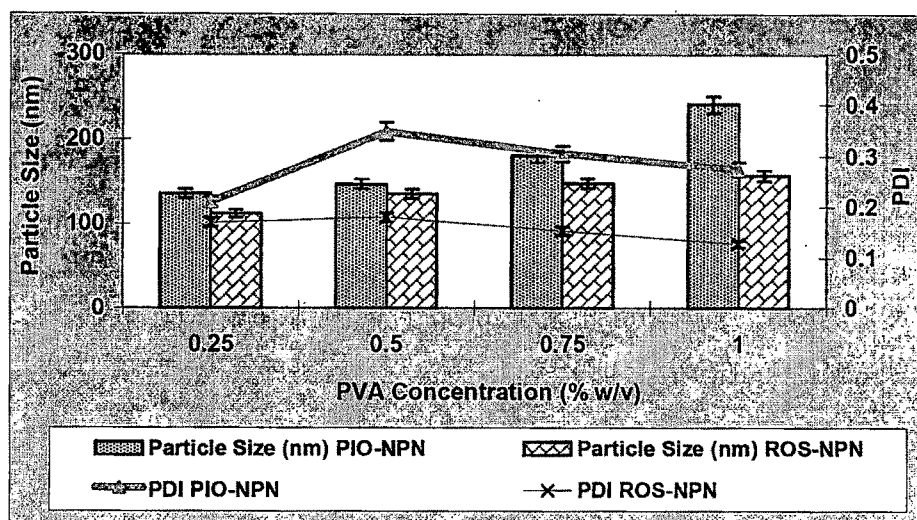


Figure 5.7: Optimization of PVA concentration with respect to particle size and PDI

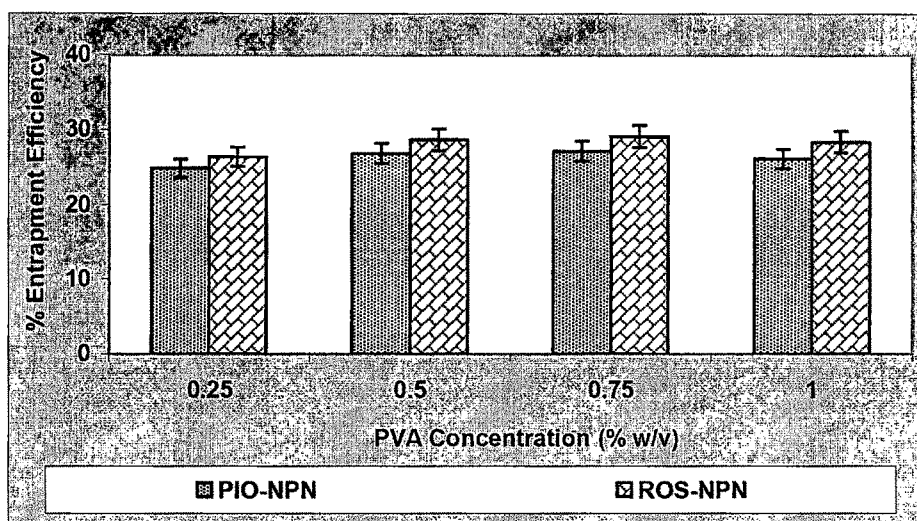


Figure 5.8: Optimization of PVA concentration with respect to entrapment efficiency

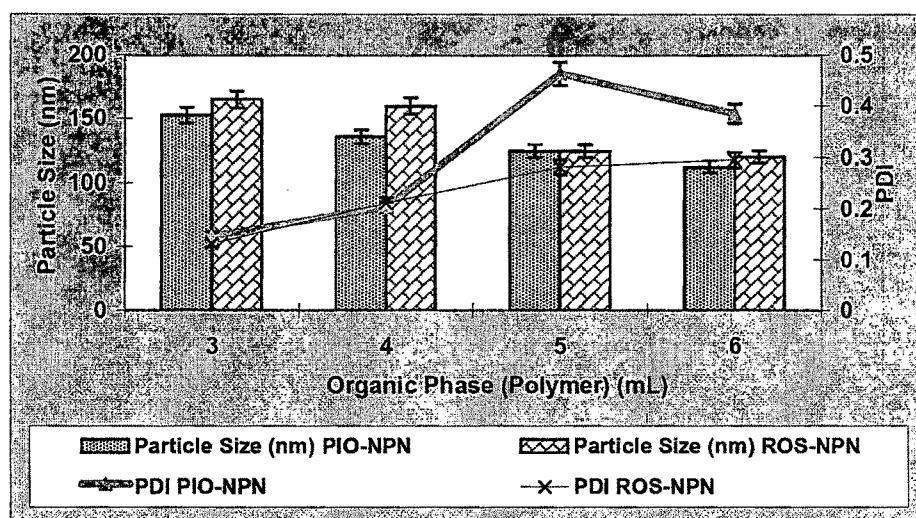


Figure 5.9: Optimization of volume of organic phase for polymer with respect to particle size and PDI

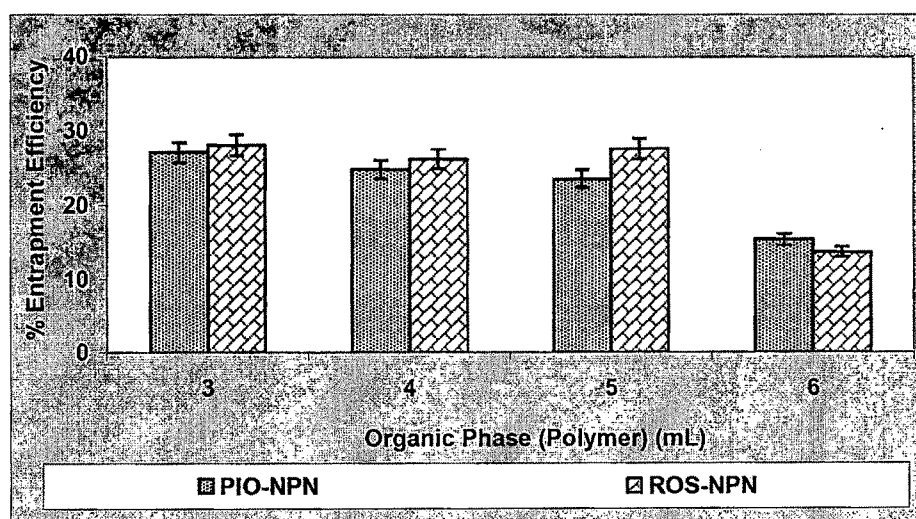


Figure 5.10: Optimization of volume of organic phase for polymer with respect to entrapment efficiency

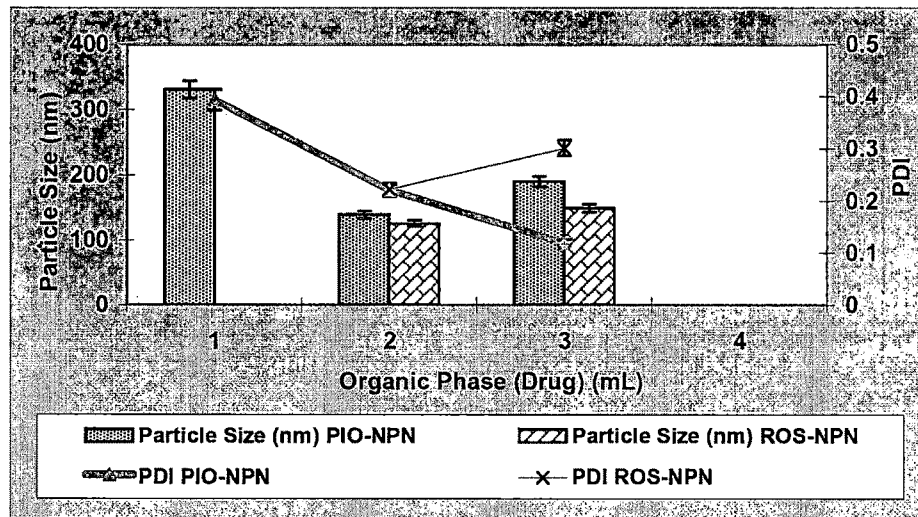


Figure 5.11: Optimization of volume of organic phase for drug with respect to particle size and PDI

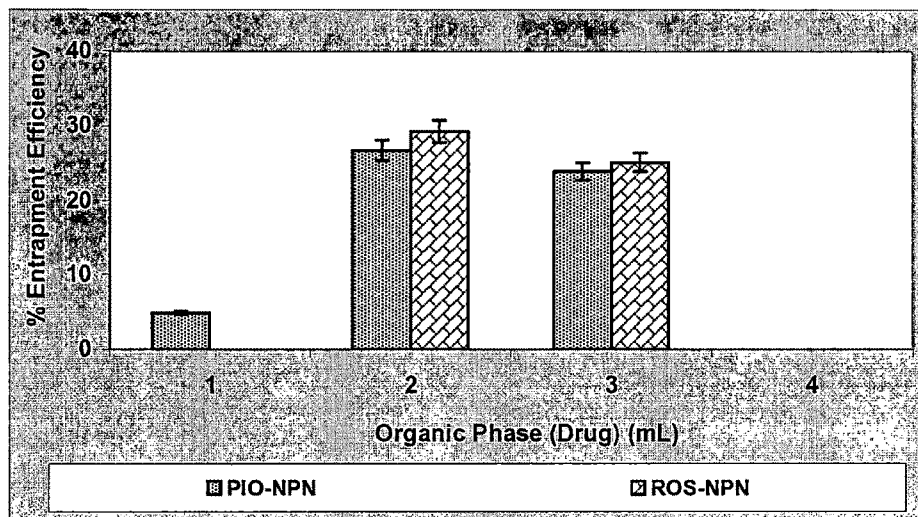


Figure 5.12: Optimization of volume of organic phase for drug with respect to entrapment efficiency

5.1.3 Emulsion Solvent Evaporation Method

PLGA nanoparticles were also prepared by emulsion solvent evaporation method reported by Tobio *et al.* (1998) with certain modifications. The basic process parameters like rate of addition of organic phase, stirring speed, volume of aqueous phase, stirring time and sonication parameters like sonication cycle, amplitude and time of sonication were standardized before proceeding for the optimization of the formulation variables. Rate of addition of organic phase was kept at 0.5 mL/min throughout the optimization process. These process parameters were standardized using qualitative examination of nanoparticles dispersion of placebo batches without drug.

Pioglitazone loaded PLGA nanoparticles (PIO-NPE) by emulsion solvent evaporation method were prepared as follows. Briefly, polymer (corresponding to 0.1 - 0.4% w/v of aqueous phase) was dissolved in ACN (0 - 3 ml) and drug (PIO, 1 - 4mg) was dissolved in a mixture of MeOH (0 - 0.5 ml) + DCM (0 - 2.0 ml). Drug solution was added to the polymer solution and this mixed solution (polymer + drug) was emulsified into 10 mL of aqueous phase containing 0 - 0.2% w/v PVA, 0 - 0.3% PLX and 0-0.01 % w/v Tween20. The emulsification was carried out by sonication using a microtip probe sonicator (Sartorius Labsonic®M Probe Sonicator, Germany) at 0.6 sec cycle and 80 amplitude for 3.5 min over an ice bath. The emulsion thus formed was stirred for 5 hrs at RT on a magnetic stirrer to allow evaporation of organic phase.

The colloidal dispersion so formed was centrifuged at 3000 rpm for 15 min at 18°C to remove untrapped drug. The supernatant was removed and again centrifuged at 11,000 rpm for 15 min at 2°C, washed thrice with distilled water to remove excess PVA. The pellet was suspended in PBS (pH 7.4) by sonication and vortexing and preceded for further characterization.

ROS loaded nanoparticles (ROS-NPE) were also prepared using the same procedure and process & formulation variables as with PIO-NPE with minor modifications such as organic phase for polymer was used as chloroform and the organic phase for drug was DCM (0 - 3.0 ml) with sonication time as 3.0 min.

5.1.3.1 Optimization

Nanoparticulate formulations were optimized for formulation variables like amount of polymer (PLGA), loading drug amount, concentration of surfactant (Tween 20) and stabilizers i.e. PVA and PLX. Concentration of PLGA was varied from 0.1-0.4% w/v of aqueous phase while keeping the other parameters constant. Subsequently amount of drug (PIO/ROS, 1-4 mg, Tween20 concentration (0 - 0.01%), PVA concentration (0 - 0.2%), PLX concentration (0 - 0.3 %) and further organic phase for polymer (0 - 3ml) and drug (0 - 3 ml) were studied (Table 5.3 & 5.4 and Fig. 5.13 - 5.28)

After analysis of results of optimization process for drug loaded nanoparticles from both NP method as well as ES method, batch of nanoparticles having highest % drug entrapment with minimum particle size was selected as optimized formulation and was used for further studies. It was observed that NPs prepared from ESE method were having much higher drug entrapment efficiency as compared to NP method and hence ESE method was selected as optimum method. The drug (PIO/ROS) loaded optimized nanoparticles i.e. PIO-NPE27 and ROS-NPE26 have subsequently been represented as NP-PIO and NP-ROS respectively in future text. All the measurements were carried out in triplicate. Statistical analysis was performed on the data obtained by one-way analysis of variance (ANOVA) with Tukey-Kramer multiple comparisons post test using Graph Pad Instat™ software. Throughout the level of significance was chosen as less than 0.05 ($p < 0.05$).



Table 5.3: Optimization of formulation parameters for Pioglitazone formulations prepared by emulsion solvent evaporation method

Formulation code	PLGA Conc. (%w/v)	Amo unit of Drug (mg)	Tween20 Conc. (% w/v)	PVA Conc. (% w/v)	PLX Conc. (% w/v)	Organic Phase for Polymer (mL)	Organic Phase for Drug (mL)	Average Particle Size (nm)	PDI	Zeta Potential (mV)	% EE
PIO-NPE1	0.1	2.0	0.005	0.1	0.1	2.0	0.5 + 1.0	256.9±7	0.189	-3.8	17.6±1.2
PIO-NPE2	0.2	2.0	0.005	0.1	0.1	2.0	0.5 + 1.0	266.1±9	0.245	-5.5	35.9±1.1
PIO-NPE3	0.3	2.0	0.005	0.1	0.1	2.0	0.5 + 1.0	284.3±5	0.262	-4.2	32.6±1.4
PIO-NPE4	0.4	2.0	0.005	0.1	0.1	2.0	0.5 + 1.0	320.1±9	0.252	-3.6	33.8±0.9
PIO-NPE5	0.2	1.0	0.005	0.1	0.1	2.0	0.5 + 1.0	210.2±0.8	0.316	-4.3	43.7±1.2
PIO-NPE6	0.2	2.0	0.005	0.1	0.1	2.0	0.5 + 1.0	231.4±4	0.302	-5.2	34.1±1.3
PIO-NPE7	0.2	3.0	0.005	0.1	0.1	2.0	0.5 + 1.0	239.2±7	0.322	-3.2	17.2±0.3
PIO-NPE8	0.2	4.0	0.005	0.1	0.1	2.0	0.5 + 1.0	228.4±6	0.314	-3.2	11.9±0.7
PIO-NPE9	0.2	2.0	0	0.1	0.1	2.0	0.5 + 1.0	-	-	-	-
PIO-NPE10	0.2	2.0	0.001	0.1	0.1	2.0	0.5 + 1.0	278.4±7	0.356	-10.2	18.3±1.4
PIO-NPE11	0.2	2.0	0.005	0.1	0.1	2.0	0.5 + 1.0	221.7±8	0.341	-12.8	39.4±1.3
PIO-NPE12	0.2	2.0	0.01	0.1	0.1	2.0	0.5 + 1.0	209.4±8	0.343	-7.4	2.1±0.5
PIO-NPE13	0.2	2.0	0.005	0	0.0	2.0	0.5 + 1.0	-	-	-	-
PIO-NPE14	0.2	2.0	0.005	0.0	0.1	2.0	0.5 + 1.0	198.6±8	0.389	-6.2	8.8±0.9
PIO-NPE15	0.2	2.0	0.005	0.1	0.1	2.0	0.5 + 1.0	218.5±5	0.292	-3.4	38.1±1.6
PIO-NPE16	0.2	2.0	0.005	0.2	0.1	2.0	0.5 + 1.0	265.8±8	0.167	-3.8	22.8±0.5
PIO-NPE17	0.2	2.0	0.005	0.1	0	2.0	0.5 + 1.0	289.2±8	0.497	-4.3	22.4±0.8
PIO-NPE18	0.2	2.0	0.005	0.1	0.1	2.0	0.5 + 1.0	250.6±4	0.219	-3.9	39.5±1.2
PIO-NPE19	0.2	2.0	0.005	0.1	0.2	2.0	0.5 + 1.0	232.8±3	0.283	-4.8	19.2±1.0
PIO-NPE20	0.2	2.0	0.005	0.1	0.3	2.0	0.5 + 1.0	206.2±8	0.291	-4.1	12.8±1.3
PIO-NPE21	0.2	2.0	0.005	0.1	0.1	0	0.5 + 1.0	-	-	-	-
PIO-NPE22	0.2	2.0	0.005	0.1	0.1	1.0	0.5 + 1.0	256.9±7	0.189	-3.8	24.8±1.2
PIO-NPE23	0.2	2.0	0.005	0.1	0.1	2.0	0.5 + 1.0	223.4±4	0.343	-2.6	37.6±0.8
PIO-NPE24	0.2	2.0	0.005	0.1	0.1	3.0	0.5 + 1.0	221.9±6	0.213	-3.3	3.6±0.8
PIO-NPE25	0.2	2.0	0.005	0.1	0.1	2.0	0.5 + 0	323.4±10	0.328	-6.7	1.5±0.9
PIO-NPE26	0.2	2.0	0.005	0.1	0.1	2.0	0 + 1.0	236.6±7	0.107	-4.8	19.9±1.2
PIO-NPE27	0.2	2.0	0.005	0.1	0.1	2.0	0.5 + 1.0	225.8±10	0.332	-11.2	41.3±1.3
PIO-NPE28	0.2	2.0	0.005	0.1	0.1	2.0	0.5 + 2.0	282.1±12	0.501	-3.8	43.5±0.9

‘-’ indicates no nanoparticle formation; Average particle size, PDI, Zeta potential and %EE values are average of 3 values ; p<0.05

Table 5.4: Optimization of formulation parameters for Rosiglitazone formulations prepared by emulsion solvent evaporation method

Formulation code	PLGA Conc. (%w/v)	Amo unit of Drug (mg)	Tween 20 Conc. (% w/v)	PVA Conc. (% w/v)	PLX Conc. (% w/v)	Organic Phase for Polymer (mL)	Organic Phase for Drug (mL)	Average Particle Size (nm)	PDI	Zeta Potential (mV)	% EE
ROS-NPE1	0.1	2.0	0.005	0.1	0.1	2.0	1.0	302.8±12	0.305	-9.33	13.5±1.5
ROS-NPE2	0.2	2.0	0.005	0.1	0.1	2.0	1.0	441.5±18	0.652	-10.6	33.6±1.0
ROS-NPE3	0.3	2.0	0.005	0.1	0.1	2.0	1.0	369.2±6	0.492	-12.2	26.3±1.0
ROS-NPE4	0.4	2.0	0.005	0.1	0.1	2.0	1.0	348.9±11	0.515	-12.6	8.26±0.6
ROS-NPE5	0.2	1.0	0.005	0.1	0.1	2.0	1.0	218.0±10	0.186	-19.8	41.1±1.5
ROS-NPE6	0.2	2.0	0.005	0.1	0.1	2.0	1.0	236.3±3	0.262	-12.59	32.2±0.8
ROS-NPE7	0.2	3.0	0.005	0.1	0.1	2.0	1.0	249.2±8	0.312	-14.1	19.1±0.8
ROS-NPE8	0.2	4.0	0.005	0.1	0.1	2.0	1.0	263.6±6	0.363	-13.5	2.17±0.8
ROS-NPE9	0.2	2.0	0	0.1	0.1	2.0	1.0	-	-	-	-
ROS-NPE10	0.2	2.0	0.001	0.1	0.1	2.0	1.0	289±18	0.268	-15.56	28.7±1.2
ROS-NPE11	0.2	2.0	0.005	0.1	0.1	2.0	1.0	219.8±9	0.252	-13.32	36.8±1.5
ROS-NPE12	0.2	2.0	0.01	0.1	0.1	2.0	1.0	169.2±4	0.301	-10.34	6.3±0.6
ROS-NPE13	0.2	2.0	0.005	0	0	2.0	1.0	-	-	-	-
ROS-NPE14	0.2	2.0	0.005	0	0.1	2.0	1.0	218.6±10	0.331	-16.4	7.7±0.5
ROS-NPE15	0.2	2.0	0.005	0.1	0.1	2.0	1.0	228.4±3	0.222	-14.2	38.6±0.6
ROS-NPE16	0.2	2.0	0.005	0.2	0.1	2.0	1.0	253.2±5	0.147	-13.2	24.3±0.8
ROS-NPE17	0.2	2.0	0.005	0.1	0	2.0	1.0	310.0±6	0.527	-11.3	15.5±0.7
ROS-NPE18	0.2	2.0	0.005	0.1	0.1	2.0	1.0	220.6±4	0.195	-15.1	19.5±1.2
ROS-NPE19	0.2	2.0	0.005	0.1	0.2	2.0	1.0	208.6±3	0.182	-12.5	20.8±0.8
ROS-NPE20	0.2	2.0	0.005	0.1	0.3	2.0	1.0	160.8±11	0.121	-14.23	10.4±1.0
ROS-NPE21	0.2	2.0	0.005	0.1	0.1	0	1.0	207.8±7	0.221	-15.8	11.5±0.5
ROS-NPE22	0.2	2.0	0.005	0.1	0.1	1.0	1.0	284.0±10	0.327	-10.4	2.4±0.4
ROS-NPE23	0.2	2.0	0.005	0.1	0.1	2.0	1.0	204.8±4	0.230	-13.0	34.2±0.9
ROS-NPE24	0.2	2.0	0.005	0.1	0.1	3.0	1.0	260.4±9	0.350	-14.1	4.3±0.5
ROS-NPE25	0.2	2.0	0.005	0.1	0.1	2.0	0	309.1±5	0.132	-8.9	2.5±0.6
ROS-NPE26	0.2	2.0	0.005	0.1	0.1	2.0	1.0	235.9±6	0.268	-12.3	39.4±1.4
ROS-NPE27	0.2	2.0	0.005	0.1	0.1	2.0	2.0	280.4±8	0.310	-12.1	37.3±1.3
ROS-NPE28	0.1	2.0	0.005	0.1	0.1	2.0	3.0	382.1±13	0.491	-10.8	42.5±0.9

'-' indicates no nanoparticle formation; Average particle size, PDI, Zeta potential and %EE values are average of 3 values ; p<0.05

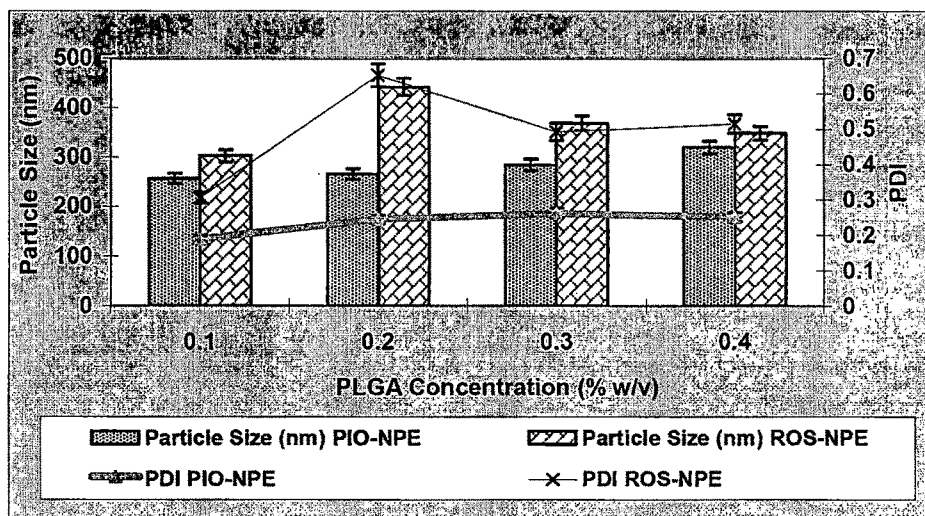


Figure 5.13: Optimization of PLGA concentration with respect to particle size and PDI

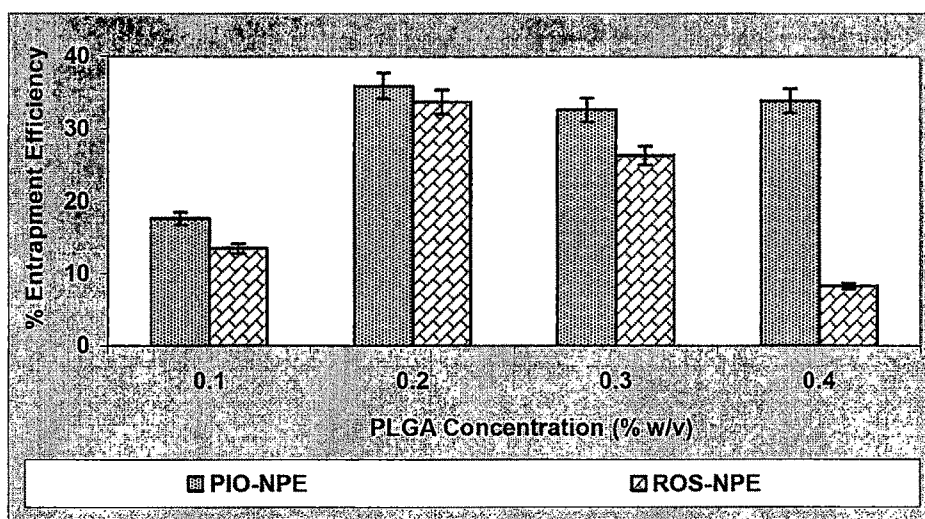


Figure 5.14: Optimization of PLGA concentration with respect to Entrapment Efficiency

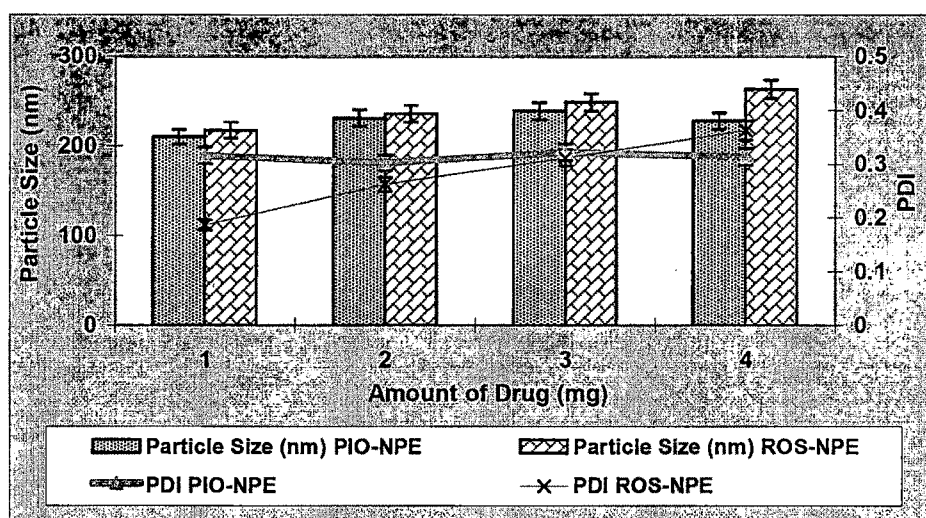


Figure 5.15: Optimization of loading amount of drug with respect to particle size and PDI

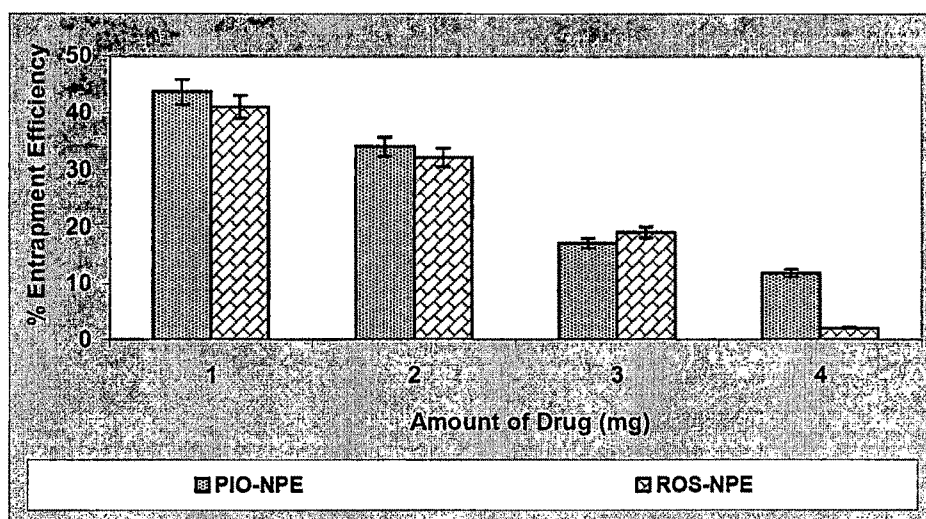


Figure 5.16: Optimization of loading amount of drug with respect to Entrapment Efficiency

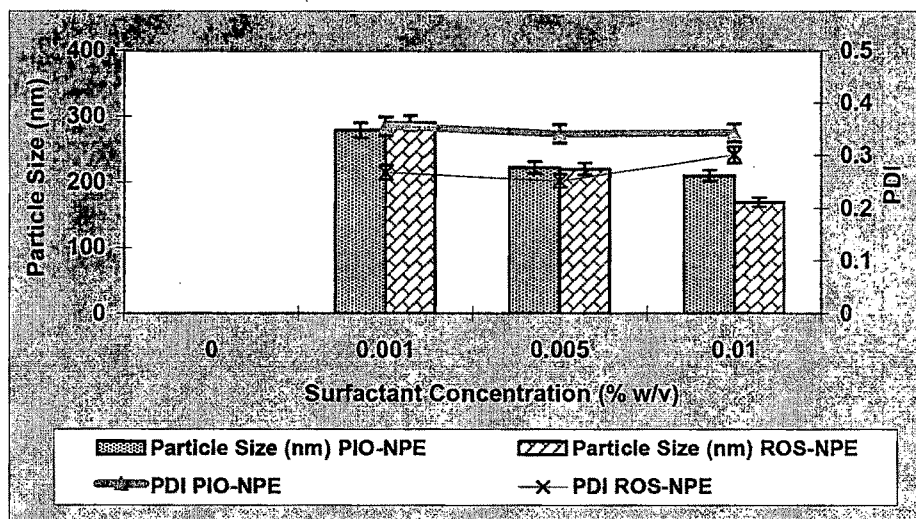


Figure 5.17: Optimization of surfactant concentration with respect to particle size and PDI

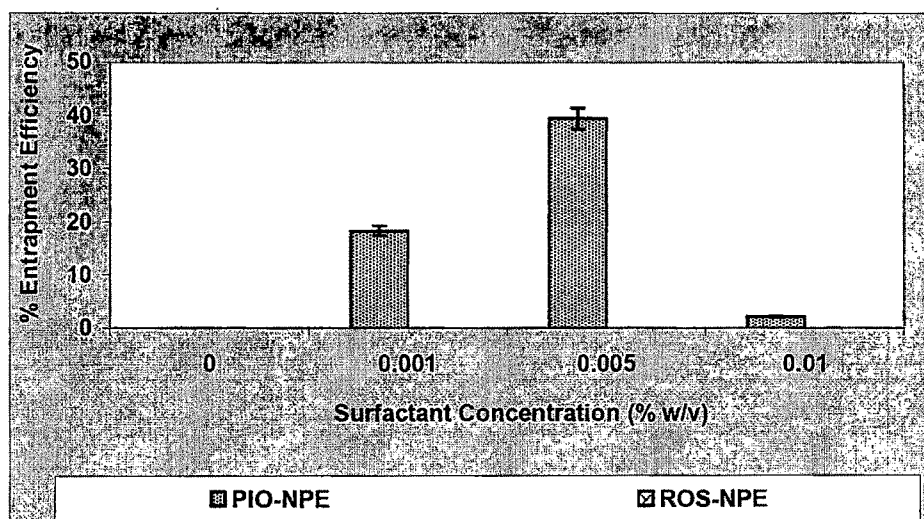


Figure 5.18: Optimization of surfactant concentration with respect to Entrapment Efficiency

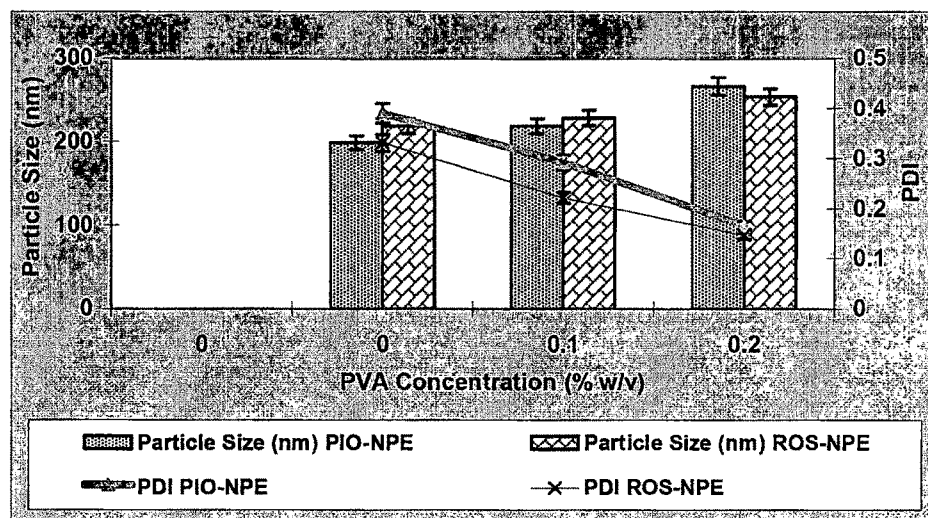


Figure 5.19: Optimization of PVA concentration with respect to particle size and PDI

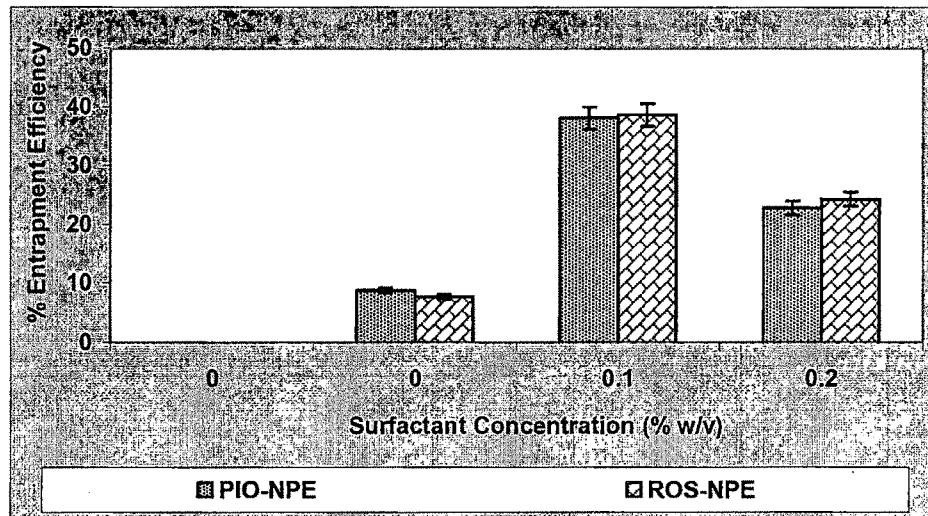


Figure 5.20: Optimization of PVA concentration with respect to Entrapment Efficiency

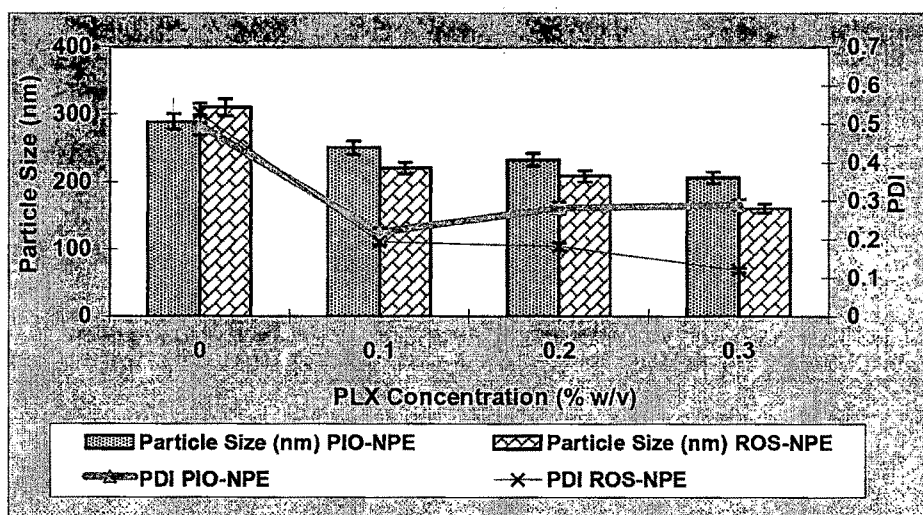


Figure 5.21: Optimization of Polaxamer concentration with respect to particle size and PDI

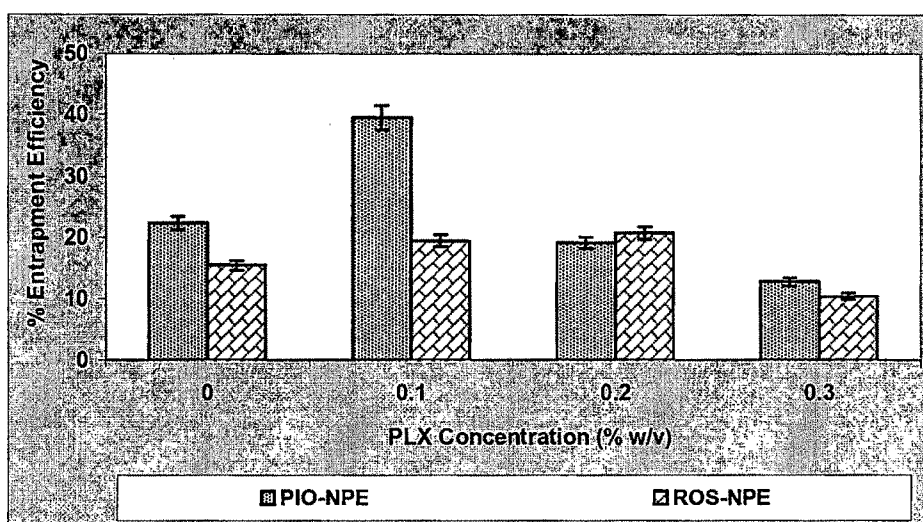


Figure 5.22: Optimization of Polaxamer concentration with respect to Entrapment Efficiency

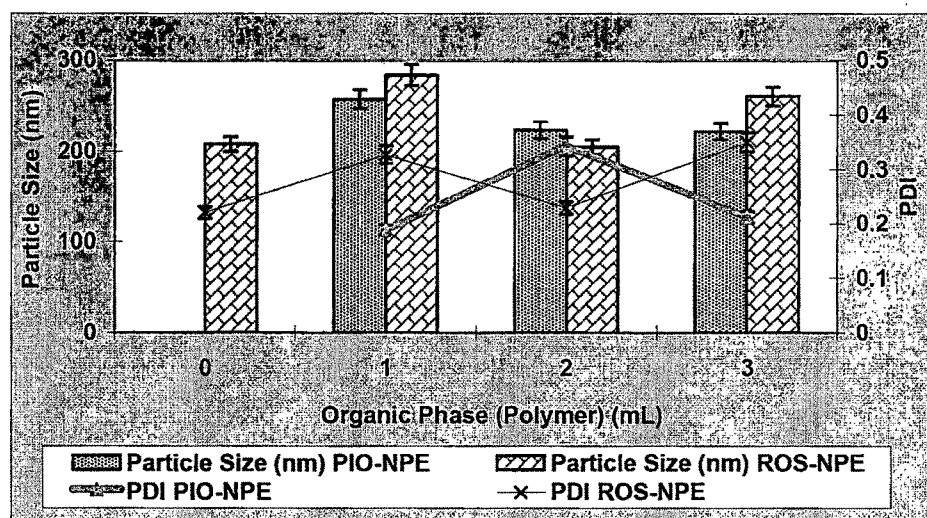


Figure 5.23: Optimization of volume of organic phase for polymer with respect to particle size and PDI

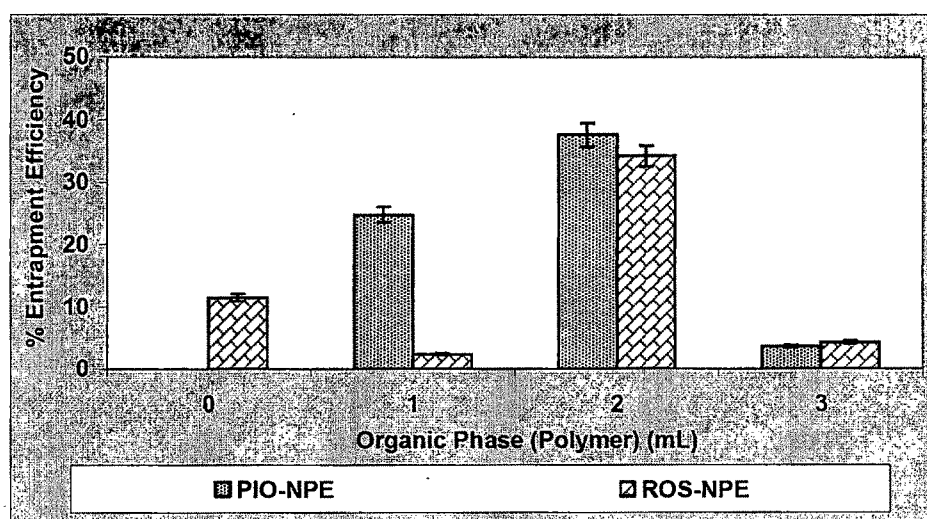


Figure 5.24: Optimization of volume of organic phase for polymer with respect to Entrapment Efficiency

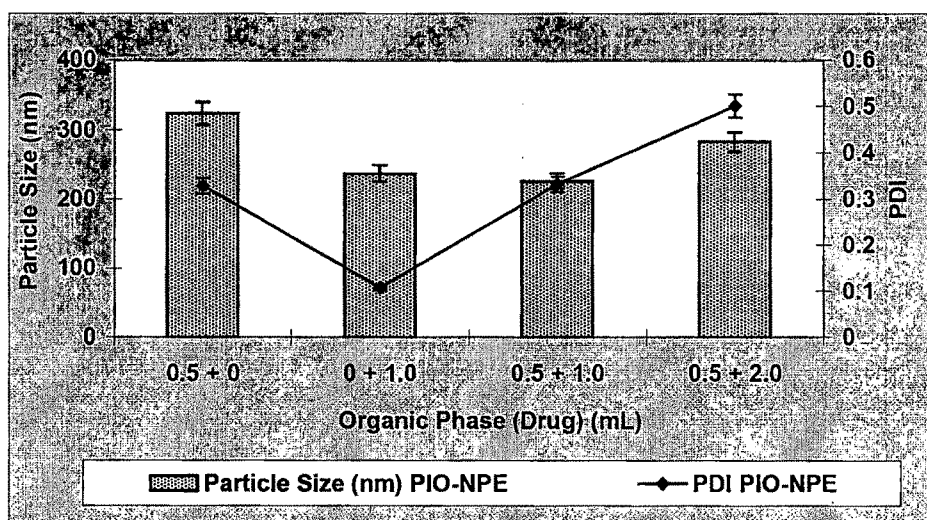


Figure 5.25: Optimization of volume of organic phase for drug with respect to particle size and PDI of Pioglitazone

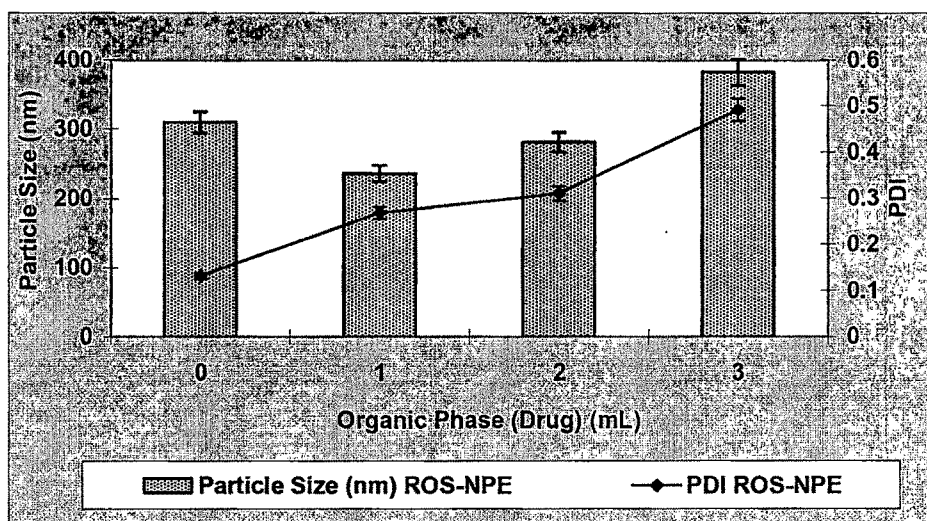


Figure 5.26: Optimization of volume of organic phase for drug with respect to particle size and PDI of Rosiglitazone

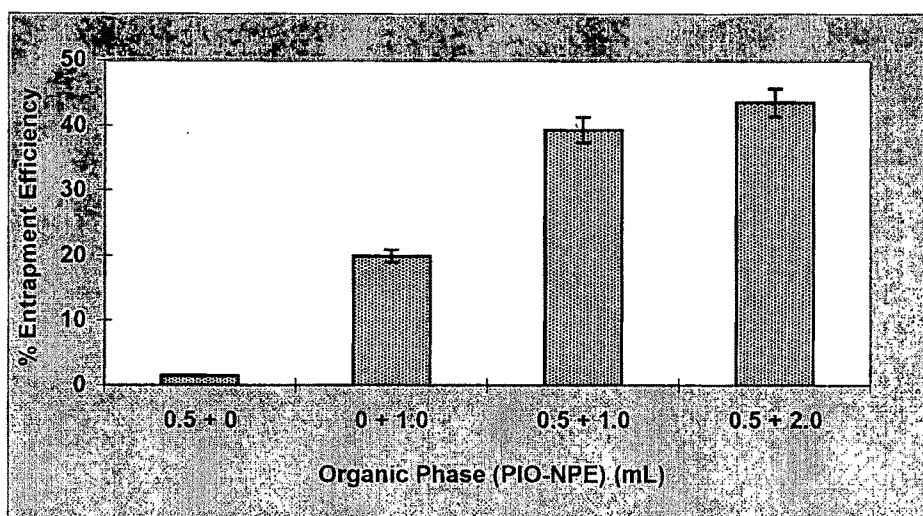


Figure 5.27: Optimization of volume of organic phase for drug with respect to entrapment efficiency of Pioglitazone

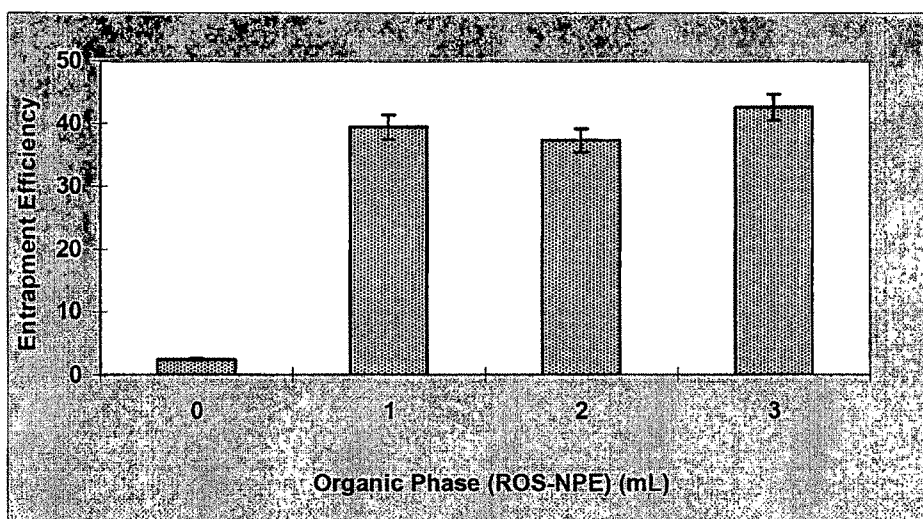


Figure 5.28: Optimization of volume of organic phase for drug with respect to entrapment efficiency of Rosiglitazone

5.2 TRANSFERRIN CONJUGATION TO NANOPARTICLES

Transferrin was coupled on to the surface of optimized nanoparticles (PIO-NP and ROS-NP) according to the method reported by Ertl et al. (2000) with slight modifications. One hundred twenty mg of drug loaded PLGA nanoparticles were suspended in PBS (pH 5.0) and activated by addition of 38.4 mg of 1-ethyl-3-(3-dimethyl amino propyl) carbodiimide (EDC). The nanoparticles suspension was stirred continuously for 0.5 h below 15°C and protected from light. Subsequently, 23 mg of N-Hydroxy succinimide (NHS) was added and the stirring was continued for another 0.5 h while maintaining the temperature below 15°C. Finally, 30 mg of transferrin was added to the suspension of activated nanoparticles and stirred for another 1.0 h below 15°C. Transferrin conjugated nanoparticles so formed were collected by centrifugation at 11,000 rpm for 15 min at 2°C and washed three times with PBS (pH 7.4) to remove uncoupled transferrin. The transferrin conjugated drug (Pioglitazone/Rosiglitazone) loaded nanoparticles are subsequently represented as Tf-PIO-NP and Tf-ROS-NP, respectively in future text of thesis.

5.3 NASAL SOLUTION

5.3.1 Nasal solution of Pioglitazone HCl (PIO-S)

Pioglitazone HCl (75 mg) was dissolved in 3.0 ml of dimethyl sulfoxide. To this solution 6.0 ml of propylene glycol was added. Simultaneously, HPMC K100LV (10 mg) was wetted with minimum quantity of ethanol and to this 1 ml of distilled water was added with continuous stirring. To the drug solution, HPMC solution was added with continuous stirring. Subsequently the formulation was filtered through 0.22 µm membrane filter and stored in air tight vials.

5.3.2 Nasal solution of Rosiglitazone Maleate (ROS-S)

Rosiglitazone maleate (15 mg) was dissolved in 10 ml of distilled water. Sodium chloride (150 mg), citric acid (34 mg) and disodium hydrogen phosphate (60 mg) were dissolved in 5 ml of distilled water to prepare 5 ml phosphate buffer saline (PBS). HPMC K100LV (20 mg) was wetted with minimum quantity of ethanol and to this 5 ml of distilled water was added with continuous stirring. HPMC solution was added to the rosiglitazone maleate solution with stirring and subsequently PBS was gradually added with stirring. The pH of the resulting solution was adjusted to pH 7.4. Further, 0.1 ml of 50% benzylkonium chloride solution was added to the above solution. Subsequently the formulation was filtered through 0.22 μ m membrane filter and stored in air tight vials.

5.4 CHARACTERIZATION OF PLGA NANOPARTICLES

5.4.1 Particle Size Measurement

Particle size was calculated on the basis of noninvasive back-scattering (NIBS) measurements using the Stokes-Einstein equation, $d(H) = kT/3\pi\eta D$. $d(H)$ is the hydrodynamic diameter, D translational diffusion coefficient, k Boltzmann's constant, T absolute temperature, and η viscosity. The diameter that is measured in DLS (Dynamic Light Scattering) refers to the particle diffusion within a fluid and is referred to as the hydrodynamic diameter corresponding to the diameter of a sphere that has the same translational diffusion coefficient as the particle.

The particle size and PDI of nanoparticulate formulations were measured using the principle of laser light scattering with zeta sizer (Nano-ZS, Malvern Instruments, Malvern, UK) and average of three measurements were recorded in **Table 5.29** for PIO-NP, Tf-PIO-NP, ROS-NP and Tf-ROS-NP, respectively.

5.4.2 Zeta Potential

The ζ potential was measured by laser Doppler anemometry-based multiple angle particle electrophoresis analyzer, Malvern Zetasizer (DTS Ver. 4.10, Malvern Instruments, Malvern, UK). The ζ potential was calculated from the electrophoretic mobility of nanoparticles based on the Helmholtz-Smoluchowski formula. All calculations were carried out by Zetasizer 4.1 software.

PIO-NP, Tf-PIO-NP, ROS-NP and Tf-ROS-NP were adequately diluted with phosphate buffer saline (PBS; pH 7.4), placed in the electrophoretic cell where an electric field of 23.2 V/cm was applied and the zeta potential was determined. The values of zeta potential were recorded in **Table 5.29** and the data represent the mean obtained for three measurements.

5.4.3 Drug Content

For determining the entrapment efficiency, it was necessary to dissolve the nanoparticles matrix, so that the total drug entrapped in the nanoparticles could be determined. The prepared nanoparticulate formulations were centrifuged at 3000 rpm for 15 min at 18°C to remove untrapped drug. The supernatant was removed and again centrifuged at 11,000 rpm for 15 min at 2°C. The pellet was washed thrice with PBS (pH 7.4) and the nanoparticle's pellet was dissolved in 1:1:1:7 ratio of mixture of methanol : acetonitrile : PBS (pH 7.4) : NaOH (0.1 N), (for PIO-NP) and in 2:3 ratio of mixture of acetonitrile : PBS (pH 7.4), (for ROS-NP), respectively. The absorbance of the resulting solution was measured at 266.0 nm and 246.2 nm for pioglitazone and rosiglitazone, respectively, taking placebo nanoparticles as blank using a UV-Visible spectrophotometer and the observations are recorded in **Table 5.29**. The absorbance of nasal solution of pioglitazone and rosiglitazone was observed at

268.0 nm and 246.8 nm against their respective blank solutions. The results are recorded in Table 5.30.

The %drug entrapment efficiency (EE) was calculated using the following equation-

$$\%EE = (\text{Amount of drug in the NPs} / \text{drug added in the formulation}) \times 100$$

5.4.4 FTIR Spectroscopy

FTIR spectroscopy of polymer (PLGA), PIO-NP, ROS-NP, Tf-PIO-NP and Tf-ROS-NP was carried out by KBr pellet technique. Small quantity of substance was mixed with potassium bromide in 1:50 ratio and was triturated with pestle-mortar. This mixture was compressed into a pellet using KBr press and was analyzed in spectroscope. The FTIR spectrum of PIO-NP, ROS-NP, Tf-PIO-NP and Tf-ROS-NP are shown in Fig. 5.29 - Fig. 5.32, respectively.

5.4.5 Morphology

The morphology of nanoparticles i.e. PIO-NP, ROS-NP, Tf-PIO-NP and Tf-ROS-NP was investigated by transmission electron microscopy (TEM) at various magnifications using Transmission electron microscope (Philips - Morgagni 268-D, Fei, The Netherlands) to determine the surface characteristics of the nanoparticles in aqueous medium using 3mm Forman (0.5% plastic powder in amyl acetate) coated copper grid (300 mesh) at 60KV using negative staining by 2% phosphotungstic acid. The TEM images of PIO-NP, Tf-PIO-NP, ROS-NP and Tf-ROS-NP are shown in Fig. 5.33 - 5.36, respectively.

5.4.6 Thermogravimetric Analysis (TGA)

Transition temperature and melting temperature of the samples i.e. pioglitazone, rosiglitazone, polymer (PLGA) and their nanoparticles i.e. PIO-NP,

ROS-NP, Tf-PIO-NP and Tf-ROS-NP nanoparticles was verified by simultaneous TG and DTA, using a Exstar TG/DTA 6300 (UK). TG-DTA curves were obtained in the temperature range from 25°C to 280°C, using aluminium crucibles with about 5 mg of samples, under dynamic nitrogen atmosphere (100 mL/min) and heating rate of 10°C/min. The thermograms are shown in Fig. 5.37 - 5.41.

5.4.7 X-ray Diffraction (XRD)

X-ray diffractograms of pioglitazone, rosiglitazone, polymer (PLGA), physical mixture of drug with polymer and their nanoparticles i.e. PIO-NP, ROS-NP, Tf-PIO-NP and Tf-ROS-NP were obtained with a X-ray diffractometer (Shimadzu XRD-6000, Japan) using Ni-filtered Cu K α radiation ($\lambda = 1.5406 \text{ \AA}$, 40 kV, 30 mA) and at a scan speed of 2°/min over a range of 10 - 60°. The x-ray diffractograms are shown in Fig. 5.42 - 5.50.

5.4.8 *In vitro* drug release from nanoparticles

In vitro drug release study was carried out by method as previously reported by Jeong et al., (1998). Ten milligrams of PIO-NP and Tf-PIO-NP were suspended in 2 mL of PBS (pH 7.4) and subsequently put into a dialysis tube (MWCO 2,000). The dialysis tube was placed into a 100 mL beaker containing 50 mL of PBS. The release media was stirred at 100 rpm and the temperature was maintained at 37 \pm 2°C. A whole-media change method was used to avoid drug saturation in the drug release study. At specific time intervals, the whole medium (50 mL) was taken and replaced with the same volume of fresh PBS (50 mL). The concentration of released pioglitazone in the PBS was determined by UV spectrophotometer at 266.0 nm.

Similarly *in vitro* drug release of rosiglitazone from ROS-NP and Tf-ROS-NP formulation's was also determined using the same experimental set up. The absorbance was noted at 246.2 nm. The results of %cumulative drug release from pioglitazone loaded nanoparticles and rosiglitazone loaded nanoparticles are shown in Fig. 5.51 and 5.52, respectively.

In vitro release data of pioglitazone and rosiglitazone from the prepared nanoparticulate formulations were applied to determine the release pattern and find out the equation with best fit release model using PCP Disso v2.08 software.

- | | | | |
|-------|---------------------------|---|--|
| (i) | Zero order | : | $%R = kt$ |
| (ii) | First order | : | $\log \% \text{ Unreleased} = kt/2.303$ |
| (iii) | Matrix (Higuchi matrix) | : | $%R = kt^{0.5}$ |
| (iv) | Peppas-Korsmeyer equation | : | $%R = ktn$ and
$\log \%R = \log k + n \log t$ |
| (v) | Hixson-Crowell | : | $(\% \text{ unreleased})^{1/3} = kt$ |

The results of model fitting were recorded in Table 5.31 - 5.34.

5.5 LYOPHILIZATION AND OPTIMIZATION OF CRYOPROTECTANT CONCENTRATION

The nanoparticles dispersion has thermodynamic instability and lead to the formation of aggregates upon storage. Freeze drying/lyophilization is one of the known techniques used to recover the nanoparticles in the dried form without affecting their thermal stability and suitably redisperse them at the time of administration. Nanoparticles suspension was added with different cryoprotectants like sucrose, mannitol and trehalose in different concentrations calculated on the basis of initial weight of formulation ingredients: cryoprotectant (CP) ratio of 1:1, 1:2, 1:3 and 1:5 before freeze-drying. The effect of

cryoprotectants and their ratio on the redispersibility and particle size of the nanoparticles after freeze-drying was investigated and recorded in Table 5.35.

Table 5.29: Particle size PDI, entrapment efficiency and zeta potential data of optimized drug (Pioglitazone/ Rosiglitazone) loaded NPs formulations

Formulation code	Average size (nm)	Polydispersity Index	% Entrapment Efficiency	Zeta Pot. (mV)
PIO-NP	225.8±10	0.332	41.3±1.3	-11.2
ROS-NP	235.9±6	0.268	39.4±1.4	-12.3
Tf-PIO-NP	394±7	0.438	29.3±1.0	-4.8
Tf-ROS-NP	389±8	0.412	29.2±1.1	-2.1

Table 5.30: Drug content of Pioglitazone/ Rosiglitazone in their nasal solution

Formulation code	Drug Content
PIO-S	99.7±1.5
RPS-S	99.8±1.2

Table 5.31: The kinetic parameters for release of Pioglitazone from PIO-NP nanoparticles in PBS (pH 7.4)

	R	K
Zero order	0.8447	0.0000
T-test	5.905	(Passes)
1st order	0.8447	0.0000
T-test	5.905	(Passes)
Matrix	0.9591	0.0002
T-test	12.681	(Passes)
Peppas	0.8174	0.0002
T-test	5.310	(Passes)
Hix.Crow.	0.8447	0.0000
T-test	5.905	(Passes)

Table 5.32: The kinetic parameters for release of Pioglitazone from Tf-PIO-NP nanoparticles in PBS (pH 7.4)

	R	K
Zero order	0.9466	0.0000
T-test	10.989	(Passes)
1st order	0.9466	0.0000
T-test	10.989	(Passes)
Matrix	0.9947	0.0001
T-test	36.220	(Passes)
Peppas	0.9554	0.0000
T-test	12.104	(Passes)
Hix.Crow.	0.9466	0.0000
T-test	10.989	(Passes)

Table 5.33: The kinetic parameters for release of Rosiglitazone from ROS-NP nanoparticles in PBS (pH 7.4)

	R	k
Zero order	0.9295	0.0001
T-test	9.428	(Passes)
1st order	0.9295	0.0000
T-test	9.429	(Passes)
Matrix	0.9962	0.0012
T-test	42.987	(Passes)
Peppas	0.9534	0.0005
T-test	11.829	(Passes)
Hix.Crow.	0.9295	0.0000
T-test	9.429	(Passes)

Table 5.34: The kinetic parameters for release of Rosiglitazone from Tf-ROS-NP nanoparticles in PBS (pH 7.4)

	R	k
Zero order	0.9450	0.0001
T-test	10.808	(Passes)
1st order	0.9450	0.0000
T-test	10.810	(Passes)
Matrix	0.9949	0.0010
T-test	36.848	(Passes)
Peppas	0.9545	0.0004
T-test	11.980	(Passes)
Hix.Crow.	0.9450	0.0000
T-test	10.809	(Passes)

Table 5.35: Effect of different cryoprotectants on the particle size and redispersability of PLGA nanoparticles

Cryoprotectant (CP)	NP : CP	Particle Size (nm)		Sr/Si	Redispersability
		Before lyophilization (S _i)	After lyophilization (S _f)		
Initial	1:0	229±6	NA	NA	NA
Sucrose	1:1	--do--	--	--	Poor Redispersability
Sucrose	1:2	--do--	727±17	3.17	--do--
Sucrose	1:3	--do--	671±15	2.93	--do--
Sucrose	1:5	--do--	410±17	1.79	--do--
Mannitol	1:1	--do--	669±15	2.92	Difficultly Redispersable
Mannitol	1:2	--do--	558±14	2.43	--do--
Mannitol	1:3	--do--	501±16	2.18	--do--
Mannitol	1:5	--do--	329±16	1.43	--do--
Trehalose	1:1	--do--	534±13	2.33	Easily Redispersable
Trehalose	1:2	--do--	482±16	2.10	--do--
Trehalose	1:3	--do--	368±8	1.60	--do--
Trehalose	1:5	--do--	317±8	1.38	--do--

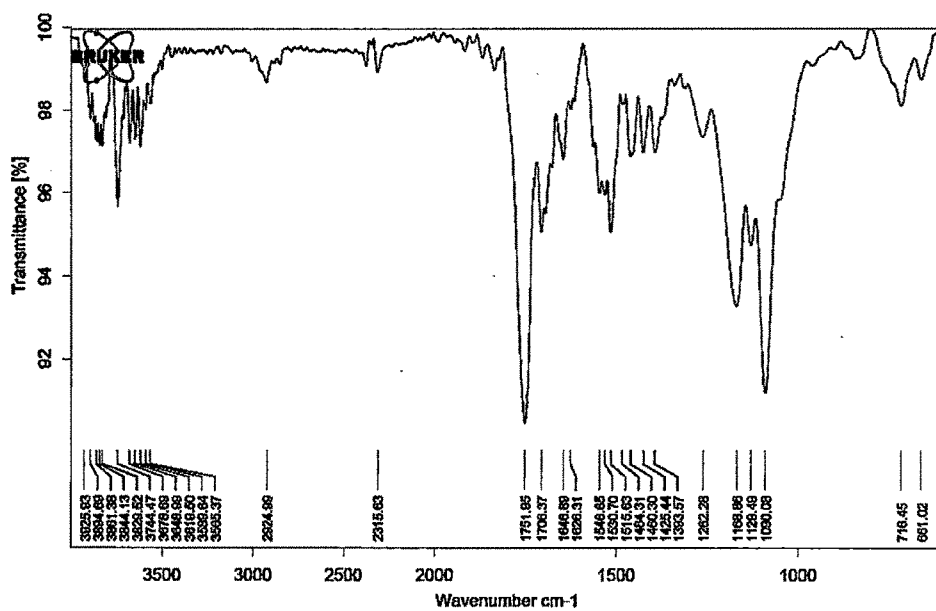


Figure 5.29: FTIR spectrum of PIO-NP

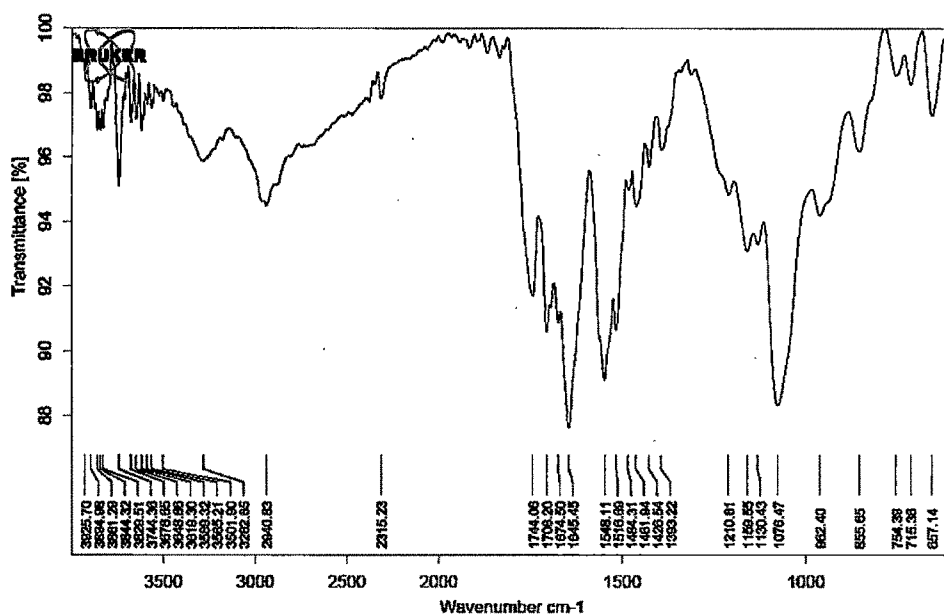


Figure 5.30: FTIR spectrum of Tf-PIO-NP

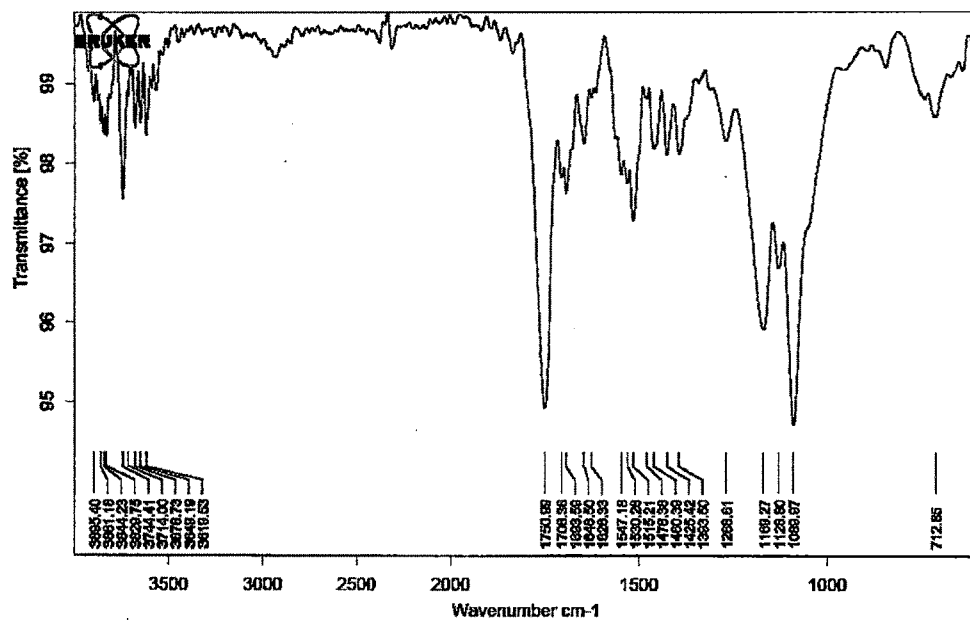


Figure 5.31: FTIR spectra of ROS-NP

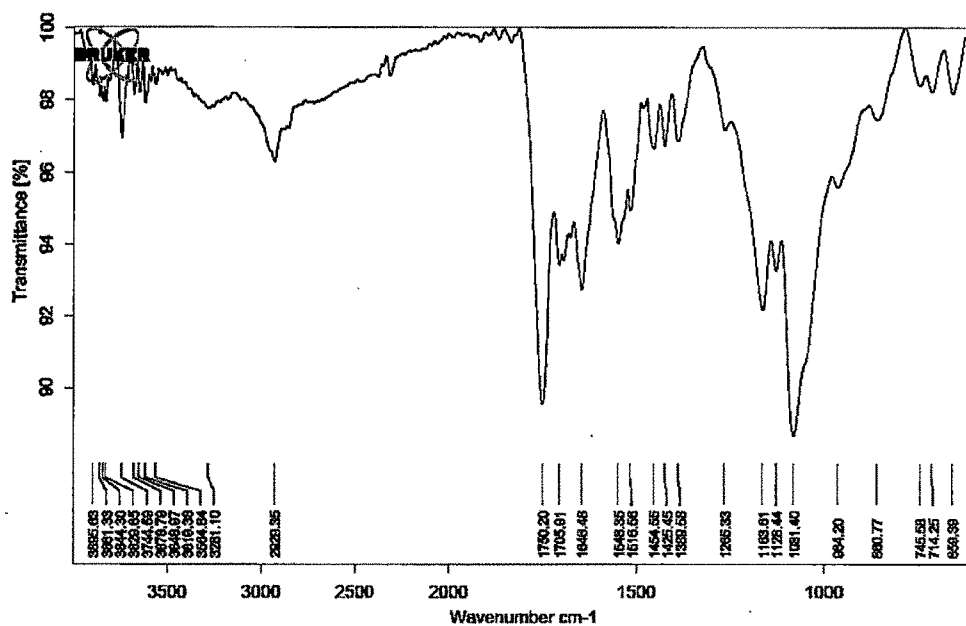


Figure 5.32: FTIR spectra of Tf-ROS-NP

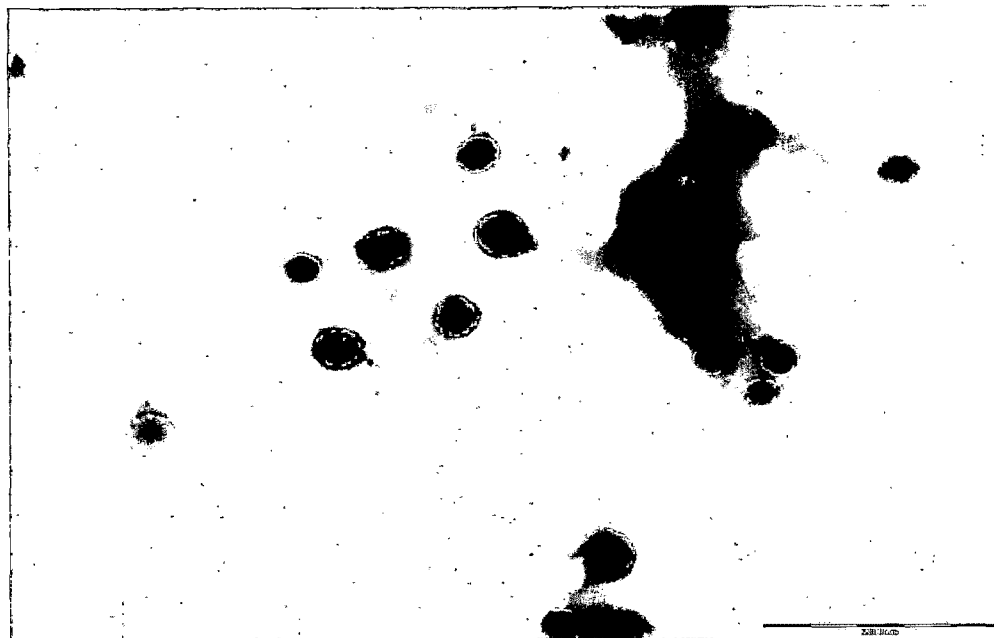


Figure 5.33: TEM Photomicrograph of PIO-NP

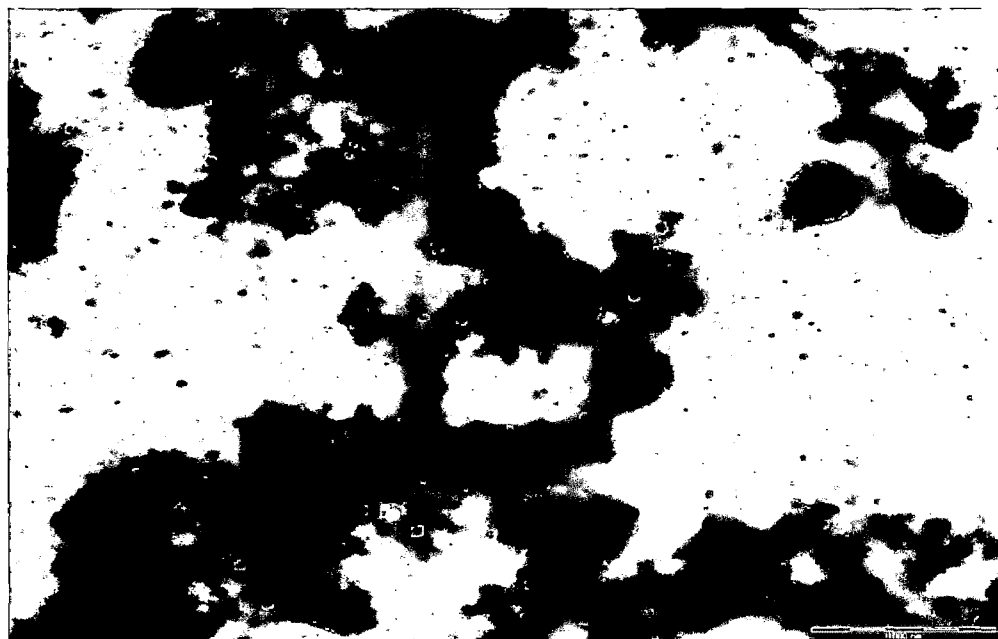


Figure 5.34: TEM Photomicrograph of Tf-PIO-NP

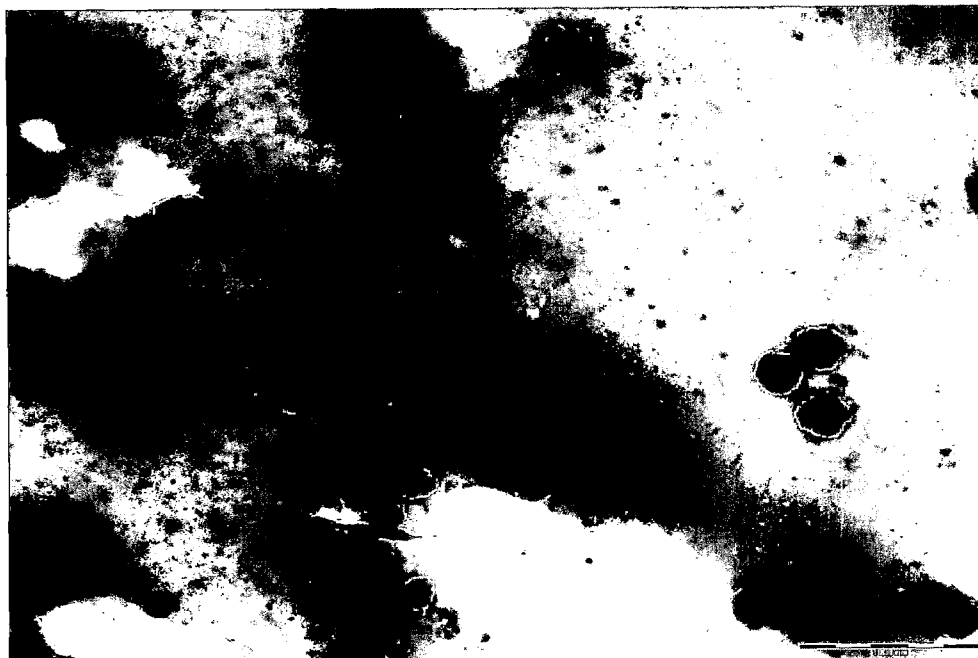


Figure 5.35: TEM Photomicrograph of ROS-NP



Figure 5.36: TEM Photomicrographs of Tf-ROS-NP

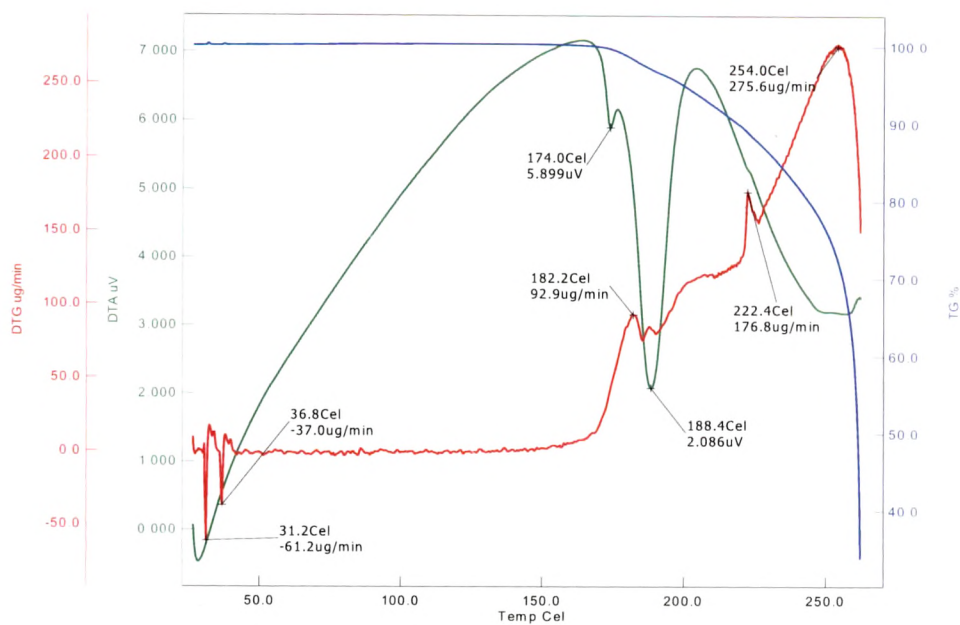


Figure 5.37: Thermogravimetric analysis of Pioglitazone

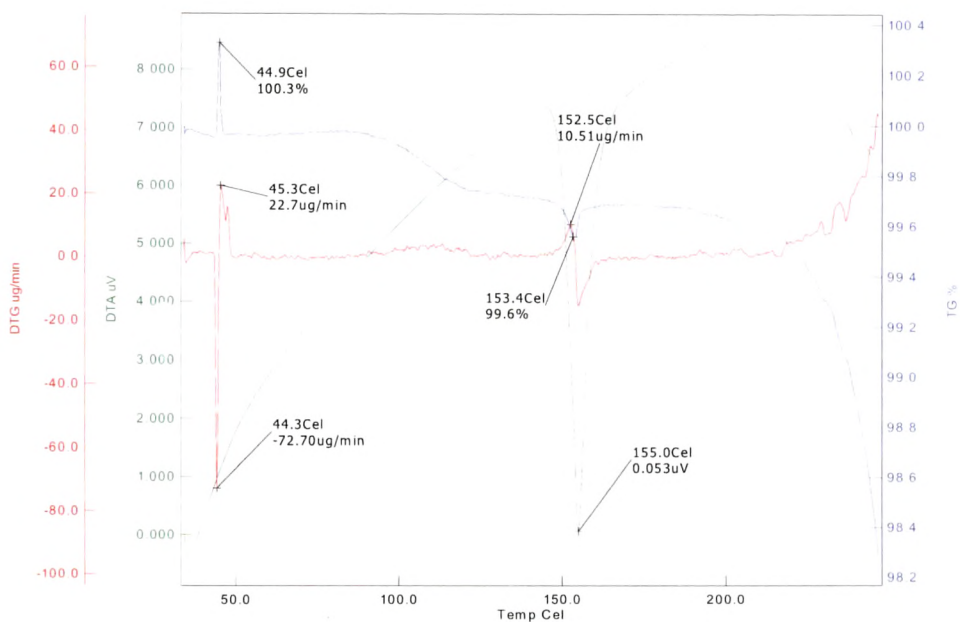


Figure 5.38: Thermogravimetric analysis of Rosiglitazone

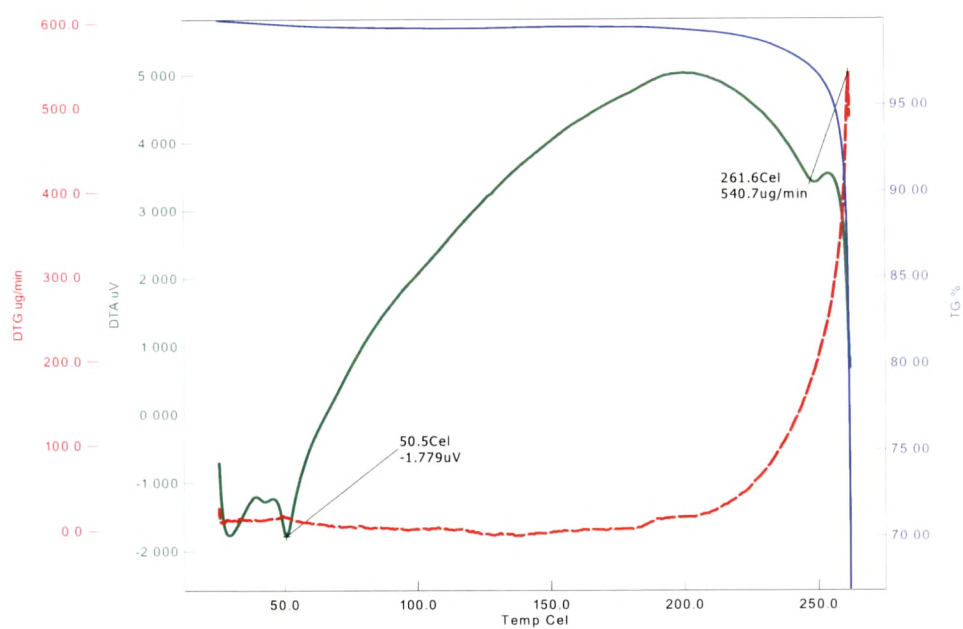


Figure 5.39: Thermogravimetric analysis of PLGA

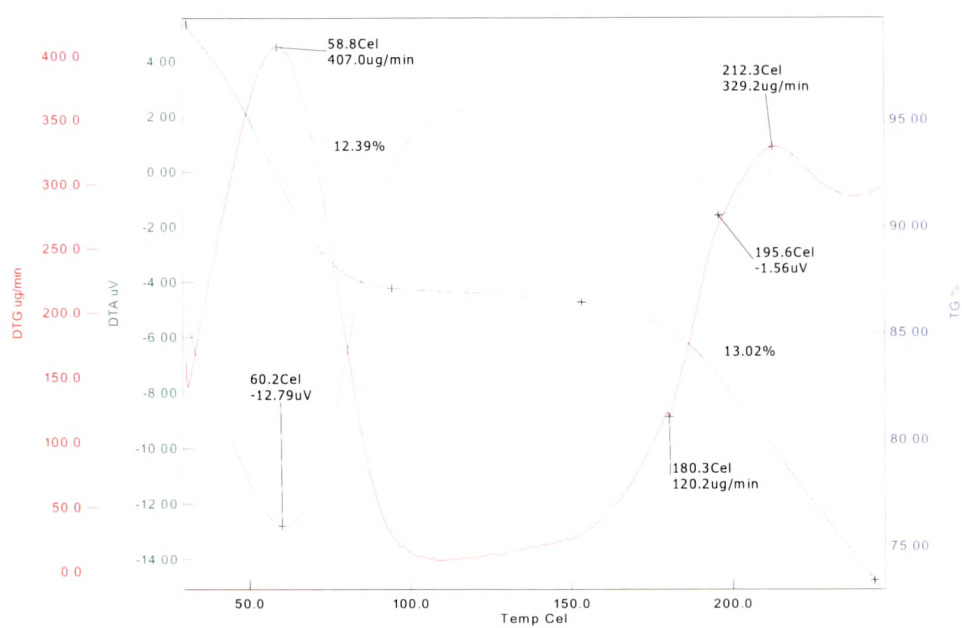


Figure 5.40: Thermogravimetric analysis of Tf-PIO-NP

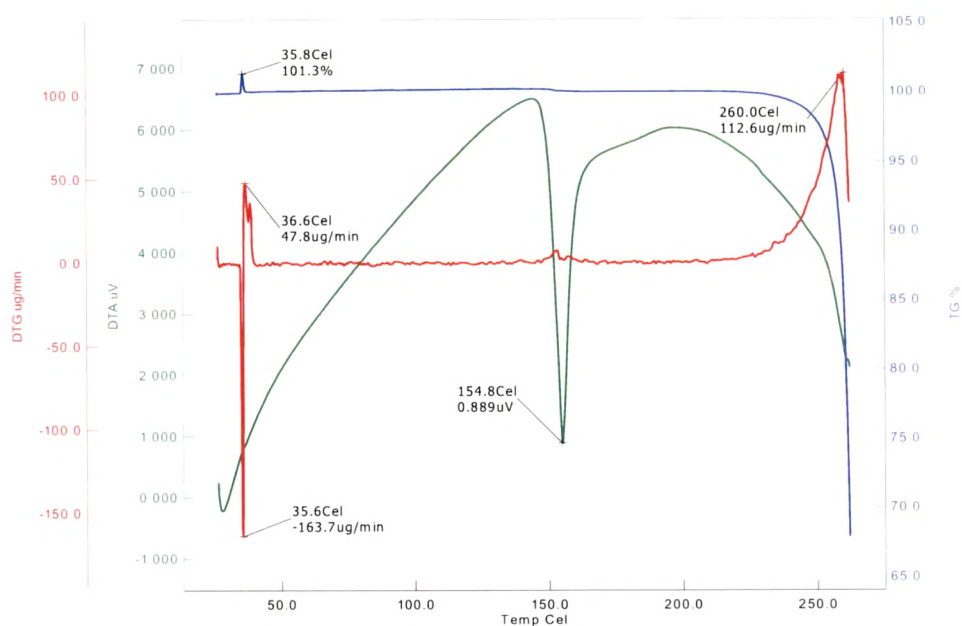


Figure 5.41: Thermogravimetric analysis of Tf-ROS-NP

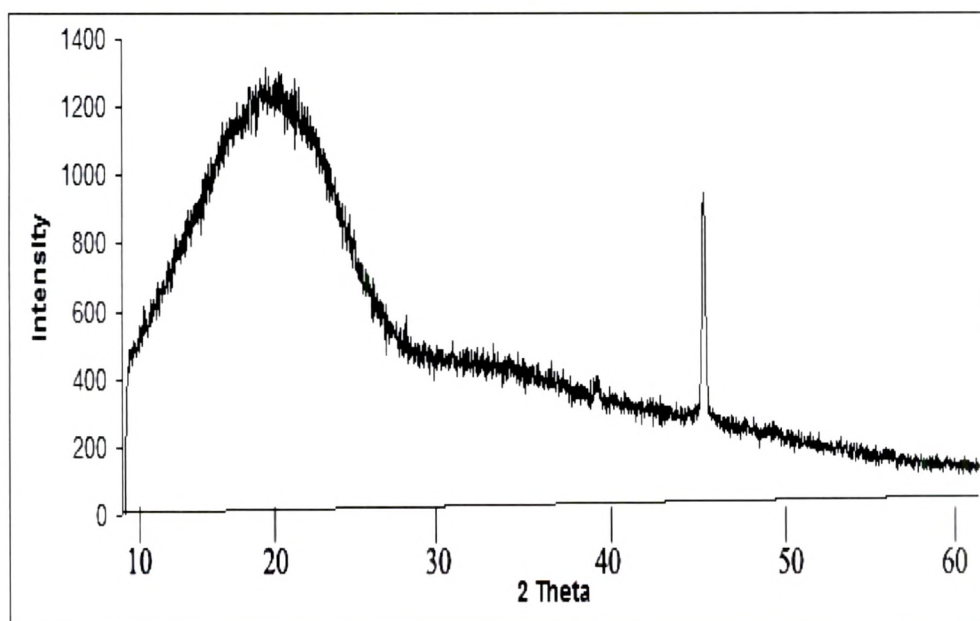


Figure 5.42: X-Ray Diffractogram of Polymer (PLGA)

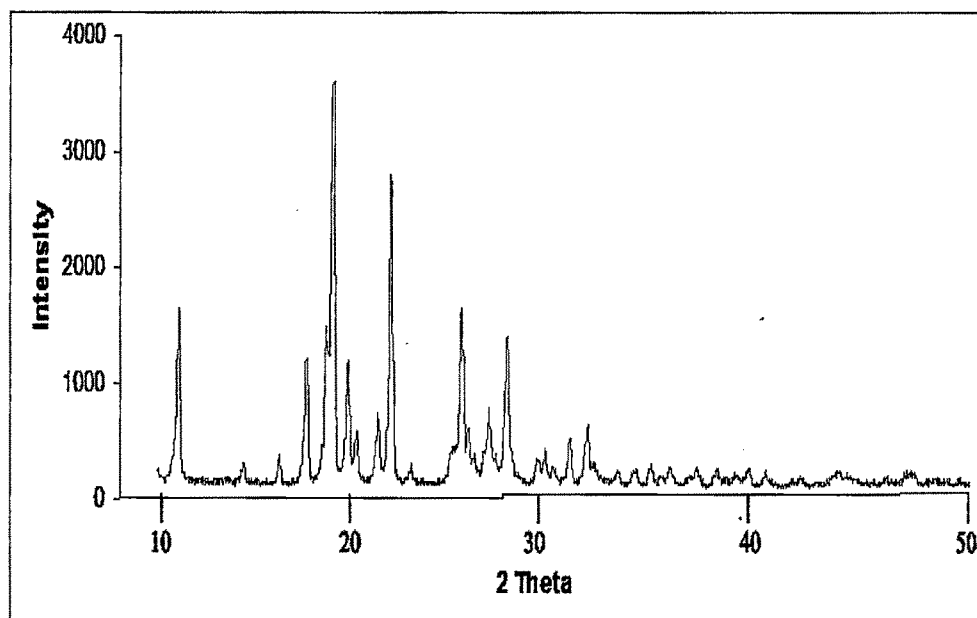


Figure 5.43: X-Ray Diffractogram of Pioglitazone HCl

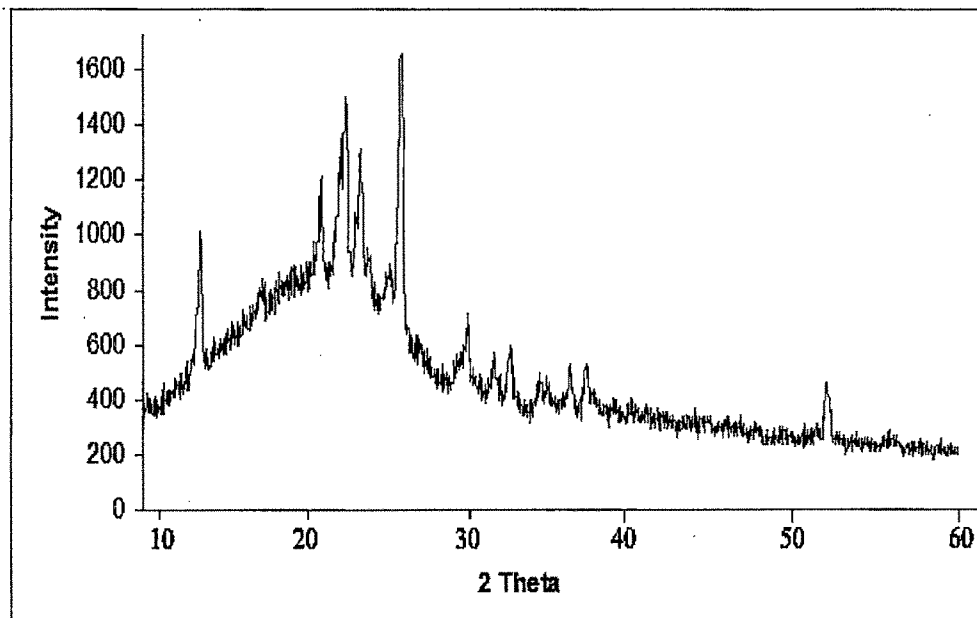


Figure 5.44: X-Ray Diffractogram of Pioglitazone-PLGA physical mixture

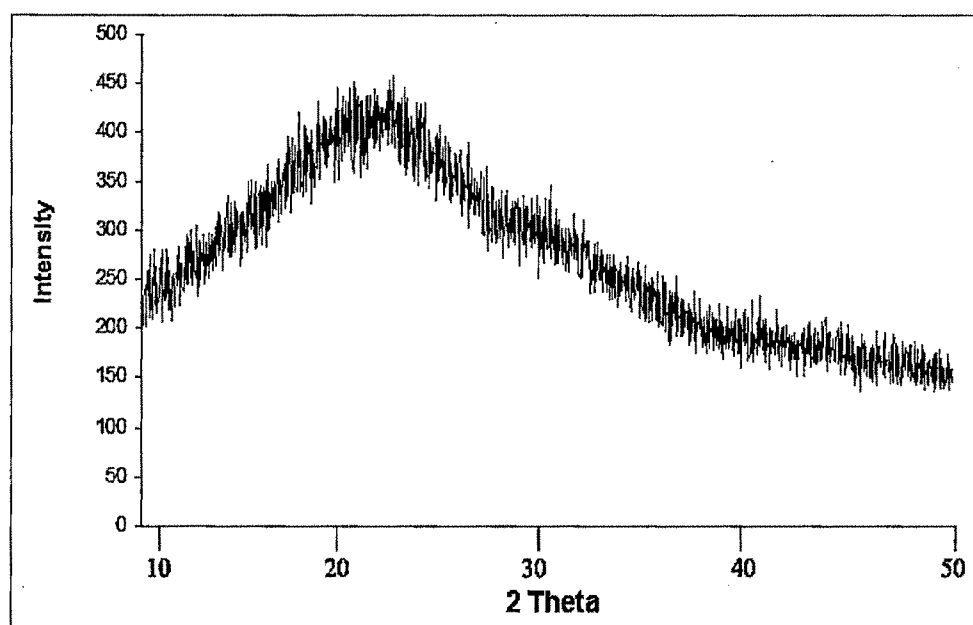


Figure 5.45: X-Ray Diffractogram of PIO-NP

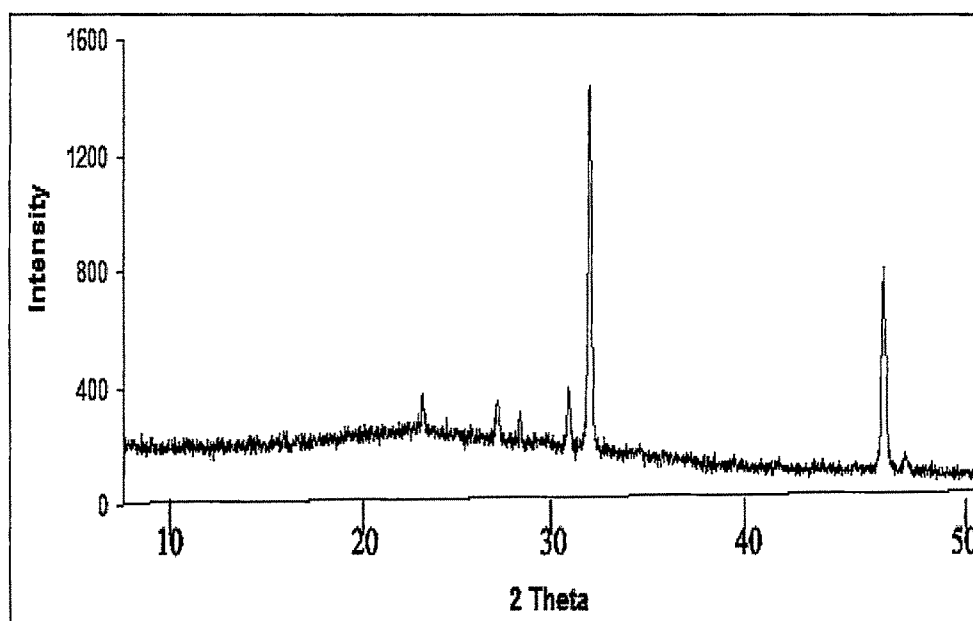


Figure 5.46: X-Ray Diffractogram of Tf-PIO-NP

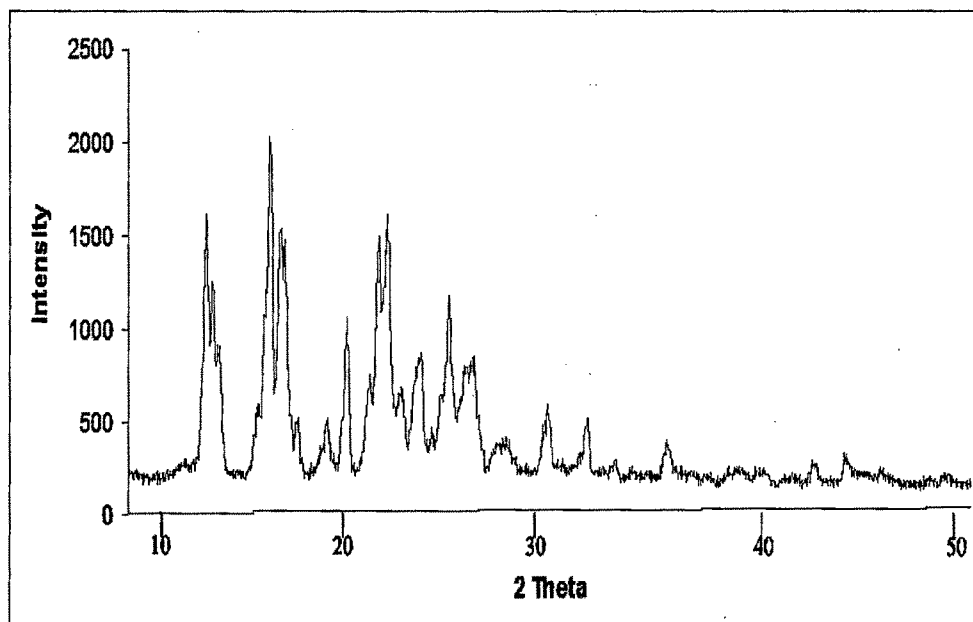


Figure 5.47: X-Ray Diffractogram of Rosiglitazone Base

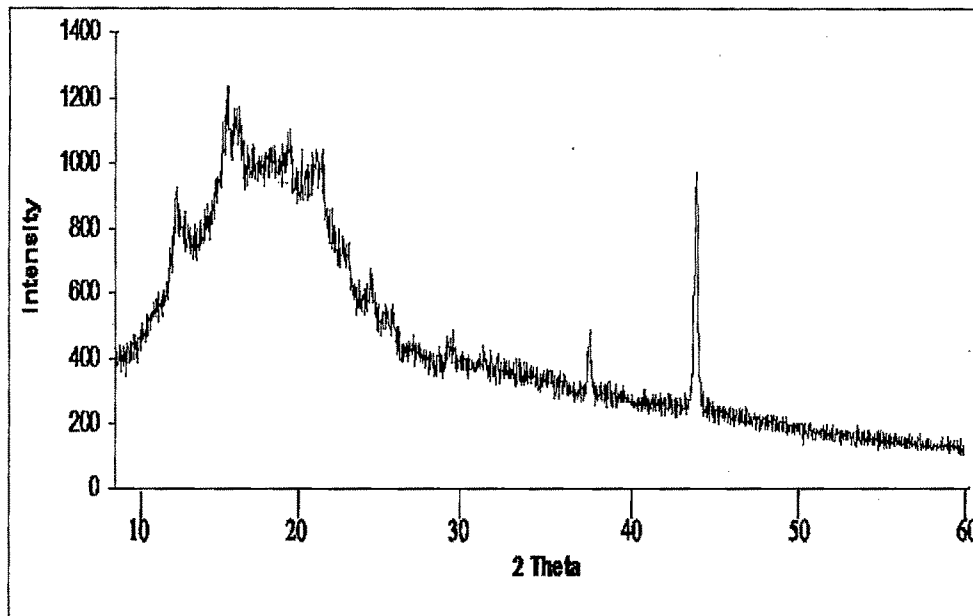


Figure 5.48: X-Ray Diffractogram of Rosiglitazone-PLGA physical mixture

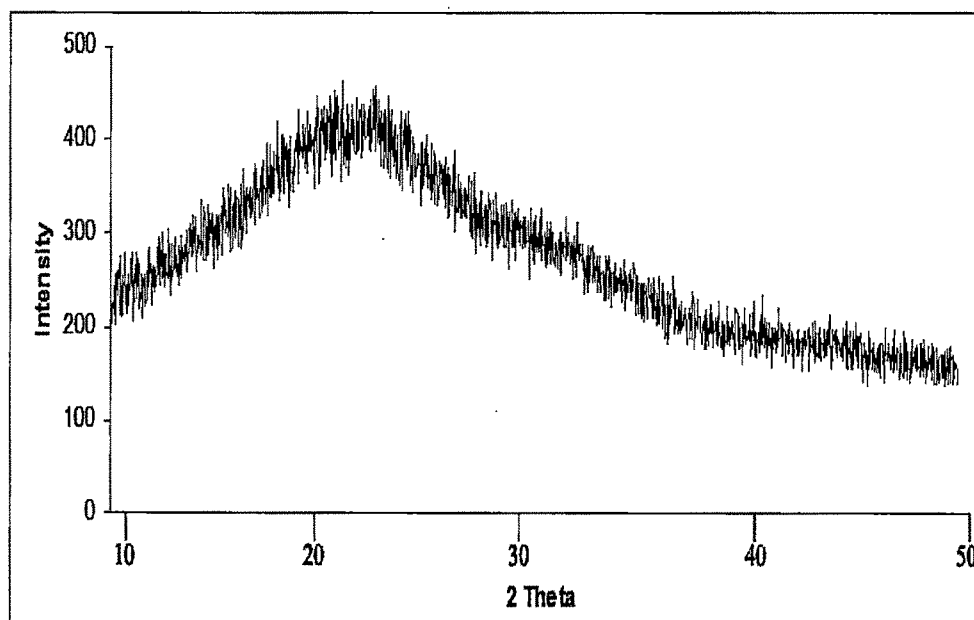


Figure 5.49: X-Ray Diffractogram of ROS-NP

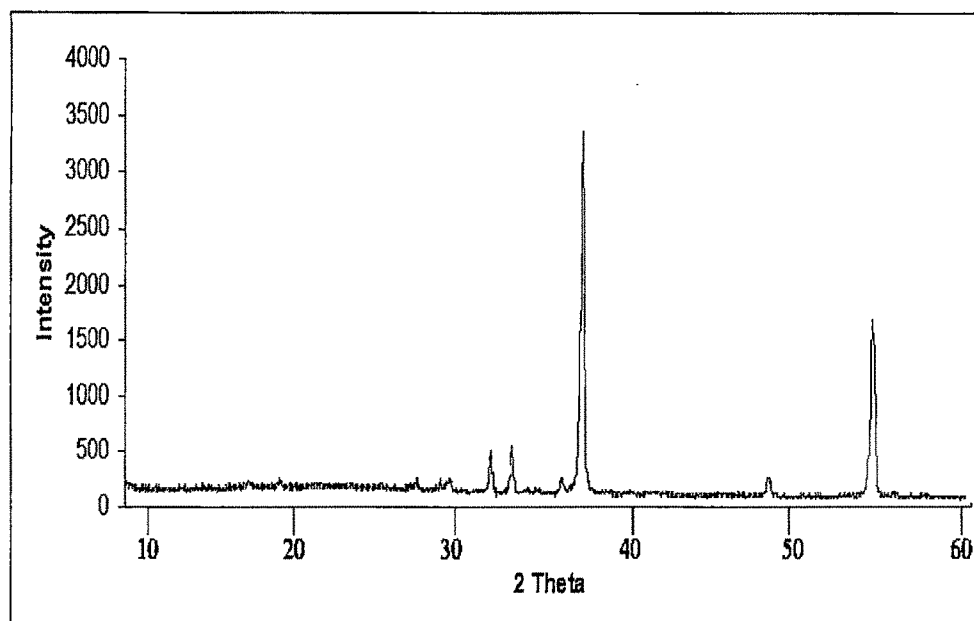


Figure 5.50: X-Ray Diffractogram of Tf-ROS-NP

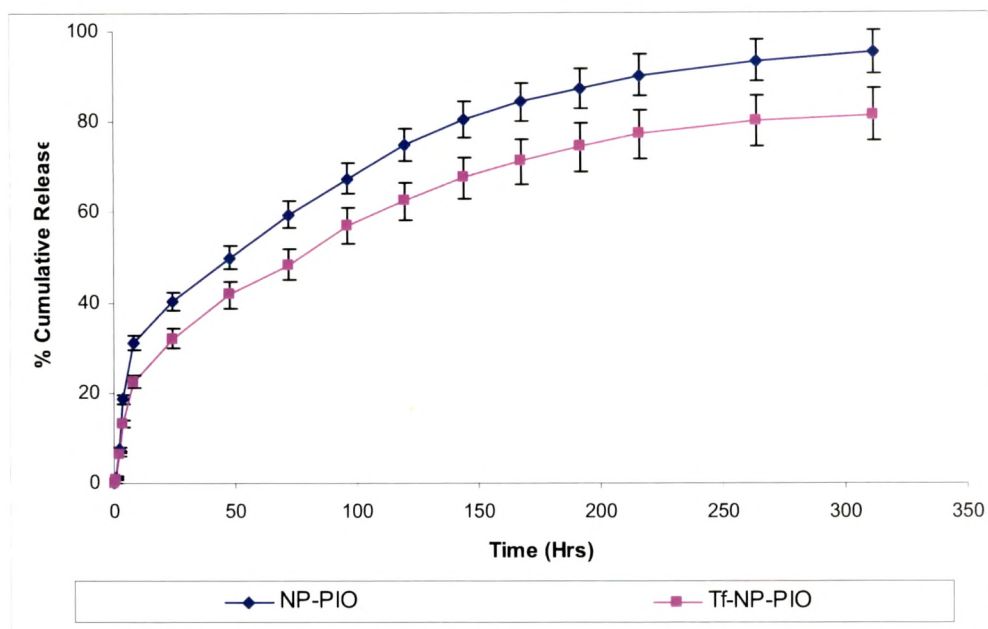


Figure 5.51: *In vitro* release profile of Pioglitazone loaded formulations

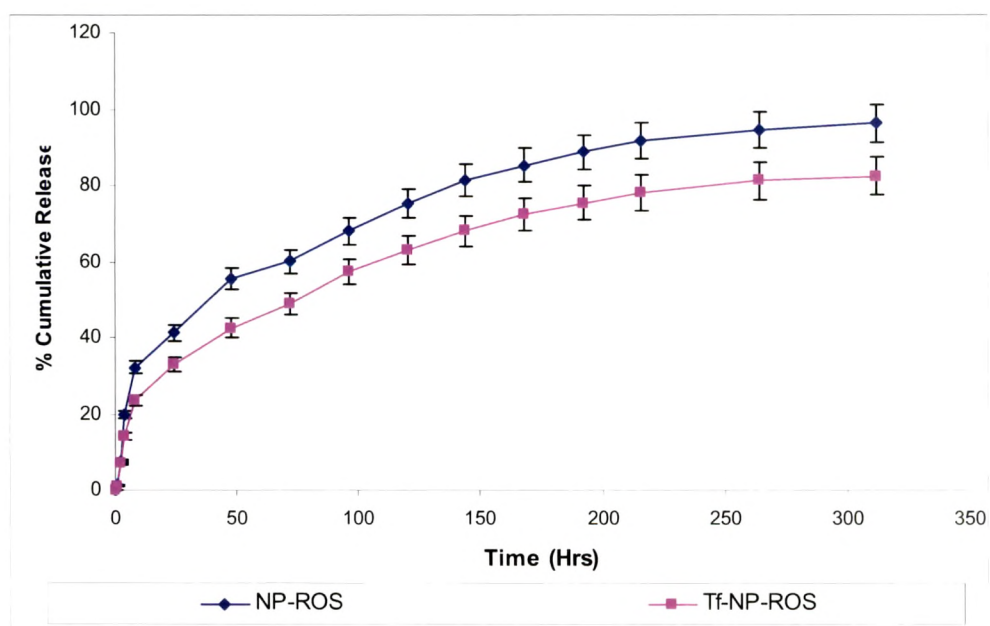


Figure 5.52: *In vitro* release profile of Rosiglitazone loaded formulations

5.6 RESULTS AND DISCUSSION

An attempt was made to study the formulation of pioglitazone and rosiglitazone entrapped nanoparticles prepared using PLGA by nanoprecipitation and emulsion-solvent evaporation method. However, these nanoparticles had no targeting potential and in order to achieve BBB targeting, some authors have attempted to increase the tissue specificity of the drug carriers by coupling targeting agents, such as monoclonal antibodies, peptide, biotin, folic acid for delivery of bioactives (Soni et al., 2008, Mishra et al., 2006)

In order to attach the targeting agents on nanoparticles, transferrin conjugates were prepared via reaction of one of the amino groups of transferrin with carboxylic groups of PLGA present on the surface of nanoparticles. By using this approach, we could successfully synthesize transferrin conjugated nanoparticles for brain targeting.

5.6.1 Optimization of the formulation variables for the preparation of nanoparticles

PLGA nanoparticles were prepared using nanoprecipitation and emulsion solvent evaporation method as reported by Fessi et al., (1989) and Vanderhoff et al., (1979) respectively, with slight modifications. The formulation method was optimized for process variables i.e. stirring speed and stirring time and also sonication cycle in ESE method. After optimization of process variables, the formulation variables including polymer concentration, loading drug amount, surfactant concentration, stabilizer concentration and volume of organic phase for polymer and drug, were optimized. In this study, drug loaded PLGA nanoparticles were to be further surface conjugated with ligand. Hence the optimization criteria for drug loaded nanoparticles were kept as minimum particle size and maximum drug entrapment efficiency.

In nanoprecipitation method, only water miscible organic solvents (such as acetone, acetonitrile) can be used for dissolving polymer (PLGA) for formulating nanoparticles, as when PLGA is dissolved in water immiscible solvents and when it is added to aqueous phase, the organic phase separates out from aqueous phase and upon their evaporation, the dissolved polymer precipitates out leading to formation of sticky mass. Also, in nanoprecipitation method, only water miscible organic solvents (such as acetone, acetonitrile, methanol and ethanol) can be used for making drug solution. Whereas, in emulsion solvent evaporation method, either water immiscible solvents or a mixture of water miscible & water immiscible solvents (such as chloroform, dichloromethane) can be utilized.

5.6.1.1 Nanoprecipitation Method: The process variables for nanoprecipitation method were optimized with placebo batches. In order to obtain particles of specific size and surface area, the effect of stirring speed was varied from 250 to 550 rpm. In case of nanoparticulate formulations, there was no significant difference in the entrapment efficiency of the batches prepared using different stirring speed and found that stirring speed did not affect the entrapment efficiency. An increase in the stirring speed from 250 rpm to 450 rpm led to a decrease in the particle. On further increasing the stirring speed to 550 rpm there was no significant decrease in the particle size. Initially the decrease in the particle size with an increase in the stirring speed may have happened due to higher energy provided at higher speed which caused the PLGA solution to be dispersed as fine droplets in the external aqueous phase thus producing particles with smaller size and narrower size distribution. Thus the stirring speed of 450 rpm was found to produce nanoparticulate formulations with a uniform size

distribution and maximum entrapment efficiency and was selected as optimum speed of stirring.

Subsequently the stirring time was optimized for the preparation of nanoparticulate formulations. Four stirring times (2 to 6 hrs) were studied in the preparation of nanoparticles in order to note the effect of evaporation of organic phase on the characteristics of the nanoparticles. Since complete evaporation of organic phase from the aqueous phase was desired hence organoleptic evaluation was performed at regular intervals to determine if traces of organic phase were not remaining in the aqueous phase. There was no significant effect of stirring time on the particle size and entrapment efficiency of the nanoparticles after 5 hrs of magnetic stirring. It was found that increase in stirring time from 3 hrs to 5 hrs led to a decrease in the particle size. Further increase in the stirring time for up to 6 hrs led to agglomeration of the nanoparticles. Thus, 5 hrs was chosen as an optimum stirring time.

Further, the nanoparticles were prepared by nanoprecipitation using different PLGA concentrations (0.1 – 0.4 %w/v of aqueous phase) (**Table 5.1 and Fig. 5.1**). The formulation PIO-NPN2 and ROS-NPN2, where 0.2% w/v PLGA concentration of aqueous phase was used as optimum polymer concentration exhibited homogenous size distribution and was selected and used for further optimization.

With the increase in entrapment efficiency, an increase in size and zeta potential were observed. However, PDI was found to decrease. The increase in size may be attributed to the entrapment of drug in the nanoparticles. The entrapment efficiency of nanoparticulate formulations increased with the increasing polymer concentration. High concentration of polymer in the internal phase could have increased the viscosity of the solution thus retarding diffusion

in effect within or through the polymeric intermediate. It may also be due to increase in drug entrapping polymer in the medium and also due to decrease in the diffusion of the drug towards the aqueous phase. However with increasing polymeric concentration in organic phase, an increase in particle size of the nanoparticles was also noticed. The increase in polymer concentration could increase the viscosity of the organic phase in which polymer is dissolved and it might have affected the size due to hindrance in rapid dispersion of PLGA solution into the aqueous phase with resulting increase in the emulsion droplet and consequently nanoparticle size. Availability of PVA in the dispersion medium adsorbs on nanoparticle's surface which prevents their mutual aggregation during solvent evaporation but at higher PLGA concentration, adsorption of PVA on the particle surface may not be uniform and sufficient leading to aggregation of particles and bigger size.

The effect of drug loading on particle size and entrapment efficiency were investigated by varying the drug loading from 1 to 4 mg in 10 ml aqueous phase. Initial drug loading in the nanoparticulate formulations was optimized by keeping the PLGA concentration constant at 0.2% w/v because it was observed to be optimum as a population of uniformly sized nanoparticle's were formed. Observations suggested that formulations **PIO-NPN6** and **ROS-NPN6** prepared by using 2 mg of drug and 0.2% w/v PLGA exhibited homogenous size distribution and maximum entrapment efficiency which were considered to be optimum and thus 2 mg drug was selected as optimum amount for loading drug. It was observed that, in case of PIO-NP initially there was an increase in encapsulation efficiency with increase in drug loading from 1 mg to 2 mg but it decreased at 3 mg and at further increase, i.e. at 4 mg loading, nanoparticles were not formed as drug got precipitated out form the aqueous phase during solvent

evaporation phase whereas in case of ROS-NP, entrapment efficiency further decreased. Hence drug amount too has a profound impact on NPs formation. Higher drug loading with PIO can cause precipitation of polymer. The reason behind this phenomenon may be related to inherent solubility of drug (PIO) in the aqueous phase at the surfactant concentration present in the aqueous phase. The surfactant at fixed concentration can solubilize a particular amount of drug in the aqueous phase, above which the excess drug precipitates out. Increasing the initial drug loading beyond inherent solubility will cause excess drug to precipitate out and will also decrease entrapment efficiency as excess drug will tend to crystallize out simultaneously initiating precipitation of solubilized drug which may have been entrapped if loading drug was low. Further increase in loading amount will cause precipitation of maximum amount of drug and this precipitated drug will disturb the equilibrium of the system and hence polymer will also precipitate out and nanoparticles will not form. Another reason for this event may be the inherent property of the polymer to entrap a fixed amount of the drug above which the excess drug will remain unentrapped and precipitates out. The minimum ratio of drug : polymer required for formulating NPs was found to be 1:10, as when this ratio was reduced, precipitation of polymer happened in conjunction with precipitation of drug due to its (drug's) low solubility in aqueous phase. The maximum loading amount of drug in nanoprecipitation method, for PIO-HCl was 3 mg whereas for ROS-B it was 5 mg, beyond these values drug precipitates out of aqueous phase.

Due to water insoluble nature of PIO-HCl, Tween 80 is required as a surfactant for entrapping the drug in PLGA NP's, in the absence of which drug gets precipitated out in aqueous phase. Tween-80 was added in the aqueous phase to improve the wetting of drugs, pioglitazone and rosiglitazone. It was

observed that at least 0.001% w/v tween-80 was required to obtain a uniform dispersion of NPs. Tween-80 concentration in aqueous phase was optimized by keeping the other parameters constant while Tween-80 concentration was varied from 0% to 0.002% w/v. The observation of results clearly shows that formulations **PIO-NPN11** and **ROS-NPN11** prepared by using 0.001 % w/v of Tween 80 exhibited homogenous size distribution and maximum drug entrapment and thus 0.001% w/v of Tween-80 was selected as optimum surfactant concentration for this method. The effect of Tween-80 concentration on the nanoparticles characteristics is shown in **Table 5.1 - 5.2** and it can be seen that there was significant effect of Tween-80 concentration on the particle size and entrapment efficiency of the nanoparticles. The particle size got reduced gradually upon increasing Tween-80 and this decrease in particle size was accompanied by initial increase in drug entrapment till 0.001% concentration and further increasing the Tween-80 concentration to 0.002% led to decrease in drug entrapment. This phenomenon may be due to the increasing surfactant action of Tween-80 which solubilized the drug more in aqueous phase leading to increase in drug entrapment but at higher concentration the solubilization was at such an extent that entrapment was reduced and hence decreased the drug entrapment.

PVA in four different concentrations (0.25, 0.5, 0.75, and 1.0% w/v of the aqueous phase) was used to optimize the stabilizer concentration required to obtain a stable colloidal dispersion. The effect of stabilizer concentration on the particle size, zeta potential, and drug encapsulation efficiency was evaluated.

Nanoparticles, because of their small size, have large surface energies, which drives the system toward aggregation. Therefore a stabilizer is required for nanoparticulate system to prevent coalescence and formation of agglomerates during and after the emulsification process. If the concentration of stabilizer is

too low, aggregation of the polymer will take place, whereas, if too much stabilizer is used, drug incorporation could be reduced as a result of the interaction between the drug and stabilizer. Increase in the PVA concentration led to increase in particle size of nanoparticles which may be due to increase in the viscosity of aqueous phase thereby increasing the resistance to the diffusion of organic phase. The miscibility of organic phase with aqueous phase results in orientation of PVA at the interface of PLGA solution in ACN present as droplets in the system (Sahoo et al., 2002). The increase in PVA concentration led to increase in particle size as well as the drug entrapment efficiency. This increase in drug entrapment efficiency may be probably due to reduction in diffusion rate of the organic phase in the aqueous phase. However, PVA did not show any concentration-dependent effect on entrapment efficiency after increasing concentration above 0.75% w/v. The stabilizer concentration was optimized at 0.25% w/v because, at higher concentration, reproducibility was compromised and also did not give any significant advantage in terms of particle size and entrapment efficiency; therefore, to maintain low stabilizer concentration without affecting the particle size or drug entrapment, nanoparticles were subsequently made using 0.25% w/v PVA. Upon scaling up the formulation parameters keeping PVA concentration constant, particle size and PDI exhibits similar values at same PVA concentration.

Keeping PVA concentration constant, when drug loading was doubled along with increase in organic phase volume, precipitation was observed; whereas reducing PVA conc. from 1% to 0.25% prevented this phenomenon (Data not shown). This can be attributed to precipitation of hydrophilic PVA in presence of organic phase which eventually disturbed the whole system leading to precipitation of PLGA. Reducing PVA concentration exposed fewer amounts

of PVA to deteriorating action of organic phase which prevented its precipitation and hence PLGA.

Upon substitution of PLX (1% w/v) for PVA as stabilizer, polymer/drug did not precipitate out even in absence of Tween 80 in the aqueous phase. PDI was significantly reduced while particle size was similar in presence or absence of Tween 80. Hence it may be concluded that Tween 80 is not required as a surfactant for entrapping PIO-HCl in PLGA NP's when 1% w/v PLX is used as stabilizer and this may be attributed to the formation of PLX micelles which possibly solubilizes and entraps the drug. It may also be a possible reason for lower entrapment efficiency of drug in the nanoparticulate formulation due to which PLX was not used as stabilizer.

The particle size and drug entrapment efficiency were found to be inversely proportional to the organic : aqueous phase ratio. As the organic : aqueous phase ratio was increased, the particle size and drug entrapment efficiency decreased. Increase in the organic phase ratio leads to increased evaporation time causing slower polymer precipitation, due to the increased microenvironment provided by organic phase after dispersing in the aqueous phase, and there by formation of small particles. Due to the increased evaporation time and slower polymer precipitation, the tendency of the drug to escape in the aqueous phase before polymer precipitation increased which lead to lower drug entrapment efficiency. Upon substitution of MeOH with EtOH as solvent for drug, magnetic stirring was required for 24 hrs to evaporate the organic phase as EtOH does not gets evaporated in usual 5 hrs period due to formation of azeotropic mixture with water. The NP's so obtained had unacceptably large particle size and PDI. Hence EtOH was not used in formulation of further batches. As ratio for drug solvent: polymer solvent was

changed from 1:2 to 2:2, precipitation of polymer took place upon mixing of two organic phases. This may have happened due to insolubility of PLGA in MeOH (organic phase for drug). Upon keeping all variables constant and doubling the polymeric organic phase no precipitation of polymer occurred, hence organic phase for polymer should always be double the amount of organic phase for drug.

5.6.1.2 Emulsion solvent evaporation method: The formulations were optimized for process variables in ESE method also. In order to obtain particles of large surface area, the effect of sonication time (1 to 4 min) was studied. A significant effect of sonication time was observed on the formation of nanoparticles as low emulsification time led to precipitation of polymer whereas high emulsification time caused decrease in entrapment efficiency. Sonication time of 3.5 min for PIO and 3 min for ROS formulations was found to produce optimum sized nanoparticulate formulations with a uniform size distribution and maximum entrapment efficiency.

The effect of stirring speed (250 to 550 rpm) was observed for the nanoparticulate formulations and stirring speed of 450 rpm was found to produce colloidal formulations of narrow size distribution, maximum entrapment efficiency and thus 450 rpm as stirring speed was used in the preparation of formulations.

The NPs prepared by emulsion solvent evaporation method were also optimized for formulation variables such as PLGA concentration, initial drug loading, surfactant concentration, stabilizer concentration, volume of organic phase and ratio of different organic phase. The formulations were prepared by taking different PLGA concentrations (0.1 - 0.4 % w/v of aqueous phase). The formulation PIO-NPE2 and ROS-NPE2 where 0.2% w/v PLGA concentration

was used as optimum concentration which exhibited homogenous size distribution and was selected and used for further studies.

Loading drug amount was optimized in the formulations by the keeping concentration of PLGA constant (0.2% w/v). The loading amount was varied from 1 - 4 mg. The observations suggested that formulations PIO-NPE6 and ROS-NPE6 prepared by using 2 mg of drug (Pioglitazone or Rosiglitazone) exhibited homogenous size distribution and maximum entrapment efficiency and therefore 2 mg drug was selected as optimum for drug loading and used in further studies.

To optimize the concentration of Tween-20 in the formulations; they were prepared by the keeping other parameters constant while Tween-20 concentration was varied (0% - 0.01% w/v of aqueous phase). On the basis of results, formulations PIO-NPE11 and ROS-NPE11 prepared by using 0.005% w/v of Tween-20 exhibited minimum particle size with maximum drug entrapment and thus 0.005% w/v of Tween-20 was selected as optimum surfactant concentration for further studies.

Formulations were subsequently optimized for stabilizer (polyvinyl alcohol) concentration (0 - 0.2% w/v). PVA acts as a stabilizer by preventing aggregation of nanoparticles and also enhance entrapment efficiency and decrease PDI. The results indicate that formulations PIO-NPE15 and ROS-NPE15 prepared by using 0.1% of PVA exhibited reasonable particle size with maximum drug entrapment and hence 0.1% PVA was selected as optimum stabilizer concentration.

It has previously been reported that use of PLX as stabilizer decreases particle size but compromises entrapment efficiency. Hence in this method, PLX in conjunction with PVA was used to get minimum particle size with high

entrapment efficiency. Effect of various concentrations of PLX (0% - 0.3% w/v of aqueous phase) on % entrapment efficiency and particle size was determined. The formulations, PIO-NPE18 and ROS-NPE18 where 0.1 %w/v PLX concentration was used as stabilizer exhibited narrow particle size distribution and was selected for further studies.

No correlation was found between particle size and drug entrapment efficiency when organic : aqueous phase ratio was increased in ROS formulation. As the organic : aqueous phase ratio for polymer was increased, the particle size decreased whereas drug entrapment efficiency initially increased and then decreased. In PIO formulations, as the organic : aqueous phase ratio for polymer was increased, correlation was found between particle size and drug entrapment efficiency.

The results clearly indicate that although nanoparticles obtained by emulsion solvent evaporation technique were of larger size as compared to nanoprecipitation technique, but significantly higher entrapment efficiency was obtained with emulsion solvent evaporation technique. Thus the later technique was selected for the preparation of nanoparticles and the nanoparticles so formed were processed to ligand conjugation and subsequent characterization studies.

The drug (pioglitazone/rosiglitazone) loaded optimized nanoparticles i.e. PIO-NPE27 and ROS-NPE26 have subsequently been represented as PIO-NP and ROS-NP, respectively in the future text of thesis.

5.6.2 Transferrin conjugation to nanoparticles

After preparation of optimized drug (pioglitazone and rosiglitazone) loaded PLGA nanoparticles i.e. PIO-NP and ROS-NP, the transferrin was

conjugated to nanoparticles. Transferrin conjugation was performed by formation of amide linkage between carboxylic groups of PLGA and amine functionalities of transferrin.

5.6.3 Characterization of PLGA Nanoparticles

5.6.3.1 Particle Size Measurement

As mentioned earlier, the particle size of nanoparticulate formulations was determined by laser diffraction particle size analyzer (DTS Ver. 4.10, Malvern Instruments, U.K.). The particle size of optimized PIO-NP was 225.8 ± 10 nm with a PDI of 0.332. Further the particle size of Tf-PIO-NP was found to be 394 ± 7 nm with a PDI of 0.438.

The particle size of ROS-NP and Tf-ROS-NP was 235.9 ± 6 nm with a PDI of 0.268 and 389 ± 8 nm with a PDI of 0.412, respectively. The results indicate nanometric size of drug loaded formulations. The results are in agreement with TEM photomicrographs which also depict an increase in size upon conjugation of ligand.

5.6.3.2 Zeta Potential

The results revealed that PIO-NP and ROS-NP exhibited a negative zeta potential of -11.2 and -12.3 mV due to negatively charged carboxylic acid groups ($-\text{COO}^-$) present at the surface of the unconjugated NP's (Table 5.29). Further, the value augmented to -4.8 and -2.1 mV in case of Tf-PIO-NP and Tf-ROS-NP. This may be attributed to conjugation of carboxylic groups with amine functionalities (NH_2) upon binding of transferrin to unconjugated nanoparticles.

5.6.3.3 Drug Content

As mentioned earlier, the drug content of nanoparticulate formulations of both drugs was determined by spectrophotometric methods and the results were recorded in Table 5.29. The drug content of Pioglitazone encapsulated in PIO-NP

and Tf-PIO-NP was found to be 41.3 ± 1.3 and $29.3 \pm 1.0\%$ respectively. Similarly, the drug content of Rosiglitazone encapsulated in ROS-NP and Tf-ROS-NP was found to be 39.4 ± 1.4 and $29.2 \pm 1.1\%$ respectively. The very close values of % drug entrapment in case of both drugs pioglitazone and rosiglitazone formulations may be due to the similar chemical structure of these molecules, both of which are thiazolidinedione derivatives. Further, the content of pioglitazone and rosiglitazone in their nasal solutions was found to be 99.7 ± 1.5 and $99.8 \pm 1.2\%$, respectively (Table 5.30).

5.6.3.4 FTIR Spectroscopy

The PLGA nanoparticulate formulations were freeze-dried without cryoprotectant and were analyzed for IR spectra by using a Fourier-transformed infrared spectrophotometer. FTIR spectra were studied in order to confirm the conjugation of transferrin to nanoparticles. PIO-NP showed the characteristic peak near 3744.47 cm^{-1} indicating $-\text{OH}$ stretching which confirms the presence of $-\text{OH}$ group, peak near 2924.99 cm^{-1} indicating $-\text{CH}-$ stretching vibration, while peak around 1751.95 cm^{-1} indicates $-\text{C}=\text{O}$ stretching and peak near 1090.08 cm^{-1} indicates the presence of $-\text{C}-\text{O}$ stretching vibration. In case of transferrin anchored nanoparticles (Tf-PIO-NP) appearance of a new characteristic sharp peak near 3501.90 cm^{-1} indicated $-\text{N}-\text{H}$ stretching which indicates the presence of amine group on the surface of PLGA nanoparticles. The intensity of peak around 1745.45 cm^{-1} indicates that $-\text{C}=\text{O}$ stretching vibration is decreased, it may be because of decrease in number of groups ($-\text{C}=\text{O}$) left in transferrin conjugated PLGA nanoparticles. The peak near 1516.69 cm^{-1} corresponds to the N-H bending vibrations for amide II and peak near 1645.45 cm^{-1} corresponding to the stretching amide I for $-\text{C}=\text{O}$ group, indicates the presence of $-\text{C}=\text{O}$ of amide group and a peak at 1210 cm^{-1} indicates $-\text{C}-\text{N}$ stretching vibration. This

confirms the formation of amide bond (-CO-NH) between ligand and carboxylic acid group of PLGA nanoparticles (Fig. 5.29 and 5.30).

Similarly, in case of ROS-NP, the FTIR spectrum showed the characteristic peak near 3744.41 cm^{-1} indicates -OH stretching which confirms the presence of -OH group, peak near 2928.65 cm^{-1} indicate -CH- stretching vibration, while peak around 1750.99 cm^{-1} indicates -C=O stretching and peak near 1089.97 cm^{-1} indicates the presence of -C-O stretching vibration. In case of transferrin anchored nanoparticles (Tf-ROS-NP) appearance of a new characteristic sharp peak near 3564.84 cm^{-1} indicated -N-H stretching which indicates the presence of amine group on the surface of PLGA nanoparticles. The peak near 1516.56 cm^{-1} corresponds to the N-H bending vibrations for amide II and peak near 1646.48 cm^{-1} corresponding to the stretching amide I for -C=O group, indicates the presence of -C=O of amide group and a peak at 1163.61 cm^{-1} indicates -C-N stretching vibration. This confirms the formation of amide bond (-CO-NH) between ligand and PLGA nanoparticles (Fig. 5.31 and 5.32).

5.6.3.5 Morphology

The shape of nanoparticles was observed under transmission electron microscope and photomicrographs were taken (Fig. 5.33 - 5.36). TEM images of the unconjugated and conjugated NPs showed spherical NPs with smooth surfaces. In the Tf-conjugated nanoparticles, a dark corona appears around the nanoparticle surface differentiating from the unconjugated nanoparticles. The results also indicate an increase in size of PLGA nanoparticles upon conjugation of transferrin ligand.

5.6.3.6 Thermogravimetric Analysis (TGA)

TGA is a very useful technique for the investigation of thermal properties of nanoparticles, providing both qualitative and quantitative information about

the presence of drug inside the nanoparticles. TGA studies were performed to investigate the physical state of the drug in the NPs, because this aspect could influence the *in vitro* and *in vivo* release of the drug from the systems as (i) amorphous drug entrapped in either an amorphous or a crystalline polymer and (ii) crystalline drug entrapped in either an amorphous or a crystalline polymer. Moreover, a drug may be present either as a solid solution or solid dispersion in an amorphous or crystalline polymer. PLGA shows a T_g and not a T_m (Melting point), indicating the presence of the polymer in amorphous form.

In the present investigation, TGA thermograms of pioglitazone, rosiglitazone, polymer (PLGA), Tf-PIO-NP and Tf-ROS-NP were taken and are shown in Fig. 5.37 - 5.41, respectively. The dips observed at temperature above 250°C might be degradation exotherm of pioglitazone, rosiglitazone, PLGA polymer, Tf-PIO-NP, Tf-ROS-NP.

The decrease in weight obtained in TGA of pioglitazone (Fig. 5.37) at 188.4°C represents the melting of pioglitazone at this temperature. Similarly, TGA of rosiglitazone base (Fig. 5.38) exhibits a decrease in weight at 155.0°C and this represents melting of rosiglitazone at said temperature. These results confirmed the authenticity of drug samples Furthermore, in case of PLGA, glass transition temperature (T_g) was obtained at 50.5°C (Fig. 5.39).

In case of TGA of Tf-PIO-NP nanoparticulate formulation, the glass transition temperature (T_g) was obtained at 60.2°C and this confirms the presence of PLGA in the nanoparticulate formulation (Fig. 5.40). Similarly, decrease in weight obtained at 195.6°C may be attributed to the melting of drug in the polymeric nanoconstructs. This showed the presence of pioglitazone and also absence of any type of physicochemical interaction of the drug with PLGA.

Similarly, TGA of Tf-ROS-NP formulation, exhibits decrease in weight obtained at 154.8°C which may be attributed to the melting of drug in the polymeric nanoconstructs (Fig. 5.41). This illustrated presence of rosiglitazone and also absence of any type of physicochemical interaction of the drug with PLGA.

5.6.3.7 X-Ray Diffraction

X-ray diffractograms reveal information on the crystal structure of different polymorphs and pseudopolymorphs. X-ray diffractograms of plain drug (Pioglitazone/Rosiglitazone), PLGA polymer, drug loaded nanoparticles and transferrin conjugated drug loaded nanoparticles were obtained with an X-ray diffractometer using Ni-filtered Cu K α radiation ($\lambda = 1.5406 \text{ \AA}$, 40 kV, 30 mA) and at a scan speed of 2°/min over a range of 10 - 60°. The XRD patterns of PLGA, pioglitazone, PLGA-pioglitazone physical mixture, PIO-NP and Tf-PIO-NP nanoparticles are shown in Fig. 5.42 - 5.46.

It may be observed that PLGA exhibits no crystalline peaks and confirms its amorphous nature whereas the XRD patterns of pioglitazone showed typical sharp peaks of drug crystals. X-Ray diffraction of physical mixture of pioglitazone and PLGA was also obtained. On comparison of XRD of physical mixture with PLGA and pioglitazone, the XRD of physical mixture clearly indicates characteristic crystalline peaks of drug and amorphous nature of PLGA. Further, XRD of PIO-NP and Tf-PIO-NP was also obtained. In case of nanoparticles loaded with pioglitazone, the specific drug crystal peaks were not observed. It may be thought that free drug crystallites exhibit sharp specific peaks when existed as drug crystals but the same drug when existed as molecular dispersion inside the nanoparticles exhibited no sharp peaks after entrapment into it. Hence possibly the drug gets dissolved during the formation of nanoparticles and subsequently gets entrapped as amorphous form.

Similar results were observed in case of Rosiglitazone loaded unconjugated and transferrin anchored PLGA nanoparticles (Fig. 5.47 - 5.50).

5.6.3.8 *In vitro* Drug Release

Since, pioglitazone and rosiglitazone were not soluble in phosphate buffer (pH 7.4), it was necessary to use a dissolution media in which the drugs are soluble and also sink conditions are maintained. Hydroalcoholic mixtures are used as dissolution media in the cases where the drugs are poorly soluble in plain buffer. Our studies indicated that the drugs are not soluble in presence of upto 30% of ethanol. Also, the ethanol could possibly dehydrate the nanoparticles leading to formation of fractures on the nanoparticles surface. Addition of surfactant to the dissolution media is a better approach to increase the solubility of the drug. Tween-80 is a commonly used surfactant in the dissolution medium. Therefore, the release studies were carried out in presence of Tween-80.

The release of drug from PLGA nanoparticles is by the degradation of the polymer by hydrolysis of its ester linkages in the presence of water. In general the mechanism by which active agent is released from a delivery vehicle is a combination of diffusion of the active agent from the polymer matrices, bulk erosion of the polymer, swelling and degradation of the polymer. The degradation of PLGA is a slow process therefore the release of pioglitazone/ rosiglitazone from nanoparticles may depend on drug diffusion from PLGA surface, bulk erosion or swelling of nanoparticles.

The release studies of pioglitazone from optimized nanoparticles batch was conducted in phosphate buffer (pH 7.4). Pioglitazone loaded nanoparticles prepared using PLGA were able to sustain the release for upto 13 days (Fig. 5.51) An initial burst release for 4 hrs was obtained. The %cumulative pioglitazone

release of 18.56 and 13.18% was obtained from PIO-NP and Tf-PIO-NP respectively, at the end of 4 hrs. This burst release may be attributed to immediate dissolution of surface adsorbed drug or the drug release from the outermost layer of the nanoparticles. Subsequently, sustained release was obtained for 13 days with a cumulative release of 95.3% and 81.4% from PIO-NP and Tf-PIO-NP, respectively. These results may be attributed to hydrophobic nature of pioglitazone that was entrapped by hydrophobic interaction of hydrophobic polymer of the polymeric nanoparticles.

Similarly, the drug release from ROS-NP and Tf-ROS-NP was found to be 96.27% and 82.51%, respectively at the end of 13 days (**Fig 5.52**). The results also indicate a decrease in drug release upon transferrin conjugation. This may be attributed to production of additional barrier to drug diffusion upon ligand conjugation. The results are in accordance with previous studies (Soni et al., 2007).

To examine the kinetics of drug release and mechanism, the release data of pioglitazone and rosiglitazone from nanoparticles were fitted to models representing zero order, first order, Higuchi matrix, Peppas-Korsmeyer, and Hixon-Crowell kinetic models, since different release kinetics are assumed to reflect different release mechanisms. Pioglitazone release from nanoparticle has suggested that release of pioglitazone from PIO-NP and Tf-PIO-NP nanoparticles followed Matrix type release pattern. In case of rosiglitazone loaded nanoparticles i.e. ROS-NP and Tf-ROS-NP also, the matrix type release model was observed (**Table 5.31 - 5.34**).

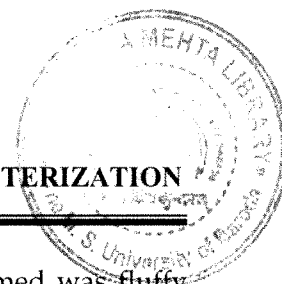
5.6.4 Lyophilization and optimization of cryoprotectant concentration

Freeze-drying, also known as lyophilization, is an industrial process which consists of removing water from a frozen sample by sublimation and

desorption under vacuum. Freeze-drying has been the most utilized drying method of nanoparticle suspension. Nevertheless, this process generates various stresses during freezing and drying steps. So, protectants are usually added to the formulation to protect the nanoparticles from freezing and desiccation stresses. For polymeric nanoparticles, carbohydrates have been perceived to be suitable freeze-drying protectants. There are considerable differences in the cryoprotective abilities of different carbohydrates. The type of cryoprotectant must be selected and its concentration must be optimized to ensure a maximum stabilization of nanoparticles.

The optimized batch of nanoparticles was lyophilized using sucrose, mannitol and trehalose (at 1:1, 1:2, 1:3 and 1:5 ratio of initial weight of formulation ingredients : cryoprotectant) in order to select suitable cryoprotectant and its concentration. The redispersibility of the freeze-dried formulations and particle size of the nanoparticles before and after freeze-drying were evaluated and recorded in **Table 5.35**.

With use of sucrose as the cryoprotectant, the cake formed after lyophilization was condensed and had collapsed structure. The redispersibility of nanoparticles with sucrose was poor and was only possible after sonication. At lowest ratio of 1:1, the lyophilized nanoparticles could not be redispersed completely. For the ratios of 1:2, 1:3 and 1:5 particle size of the nanoparticles increased significantly after lyophilization. The S_f/S_i values were 3.17, 2.93 and 1.79 with 1:2, 1:3 and 1:5 ratio of NPs: sucrose, respectively. The increase in the particle size could have been due to the cohesive nature of the sucrose. Further, it was observed that the lyophilized nanoparticles with sucrose had tendency to absorb moisture very quickly.



With mannitol, the lyophilized nanoparticles product formed was fluffy and snow like voluminous cake. With mannitol, the nanoparticle formulation showed free flowing ability, however the redispersion was difficult and possible only after vigorous shaking. The particle size, observed after lyophilization increased significantly than the initial particle size. The S_f/S_i values were 2.92, 2.43, 2.18 and 1.43 with 1:1, 1:2, 1:3 and 1:5 ratio of NPs : mannitol, respectively. This may be due to the low solubility of mannitol in water i.e. 0.18 part of mannitol is soluble in 1 part of water.

With trehalose also, the lyophilized nanoparticles formed fluffy and snow like voluminous cake. With trehalose as cryoprotectant, the lyophilized nanoparticles were redispersed easily and the increase in particle size was not remarkable as indicated by S_f/S_i values which were 2.33, 2.10, 1.60 and 1.38 for 1:1, 1:2, 1:3 and 1:5 ratio of NPs : trehalose, respectively. Redispersion of the nanoparticles depends on the hydrophilicity of the surface. The easy redispersibility is probably due to the higher solubility of trehalose in water i.e. 0.7 parts in 1 part of water. The cryoprotectant effect may be attributed to the ability of trehalose to form a glassy amorphous matrix around the particles, preventing the particles from sticking together during removal of water.

Therefore, trehalose at a ratio of 1:5 (initial weight of formulation ingredients : trehalose) was used as cryoprotectant for lyophilization of optimized batch of nanoparticles for further studies.

5.7 CONCLUSION

After characterization it may be concluded that the unconjugated and transferrin conjugated nanoparticles of pioglitazone and rosiglitazone have small particle size suitable for intravenous administration. A prolonged release was

observed for both unconjugated and conjugated nanoparticles of pioglitazone and rosiglitazone. The smooth and spherical surface of nanoparticles was confirmed from TEM. The XRD studies indicate the presence of the drug in nanoparticles in the amorphous state.

The unconjugated and Tf conjugated nanoparticles of pioglitazone and rosiglitazone were further subjected to stability studies according to ICH guidelines.

REFERENCES:

- Alexis, F., Pridgen, E., Molnar, L.K., Farokhzad, O.C. 2008. Factors Affecting the Clearance and Biodistribution of Polymeric Nanoparticles. *Mol. Pharm.* 5(4), 505-515.
- Andrews, N.C. 2000. Iron homeostasis: insights from genetics and animal models. *Nat. Rev. Genet.* 1, 208-217.
- Bickel, U., Yoshikawa, T., Pardridge, W.M. 2001. Delivery of peptides and proteins through the blood-brain barrier. *Adv. Drug Deliv. Rev.* 46, 247-279.
- Fessi, H., Puisieux, F., Devissaguet, J.P., Ammoury, N., Benita S. 1989. Nanocapsule formation by interfacial polymer deposition following solvent displacement. *Int. J. Pharm.* 55, R1-R4.
- Jeong YI, Cheon JB, Kim SH, Nah JW, Lee YM, Sung YK. 1998. Clonazepam release from core-shell type nanoparticles in vitro. *J Control Release.* 51:169-78.
- Labhasetwar, V. 1997. Nanoparticles for drug delivery. *Pharm News.* 4, 28-31.
- Li, H. and Qian, Z.M. 2002. Transferrin/transferrin receptor-mediated drug delivery. *Med. Res. Rev.* 22, 225-250.
- Li, H., Sun, H., Qian, Z.M. 2002. The role of the transferrin-transferrin receptor system in drug delivery and targeting. *Trends Pharmacol. Sci.* 23, 206-209.
- Mishra, V., Mahor, S., Rawat, A., Gupta, P.H., Dubey, P., Khatri, K., Vyas, S.P. 2006. Targeted brain delivery of AZT via transferrin anchored pegylated albumin nanoparticles. *J. Drug Target.* 14(1), 45-53.
- Pardridge, W.M. 2002. Blood-brain barrier drug targeting enables neuroprotection in brain ischemia following delayed intravenous administration of neurotrophins. *Adv. Exp. Med. Biol.* 513, 397-430.
- Qian, Z.M. and Tang, P.L. 1995. Mechanisms of iron uptake by mammalian cells. *Biochim. Biophys. Acta.* 12(69), 205-214.
- Sahoo, S.K., Panyam, J., Prabha, S., Labhasetwar, V. 2002. Residual polyvinyl alcohol associated with poly (D,L-lactide-co-glycolide)

nanoparticles affects their physical properties and cellular uptake. *J. Control. Rel.* 82, 1105-1114.

- Scholes, P.D., Coombes, A.G.A., Illum, L., Daviz, S.S., Vert, M., Davies, M.C. 1993. The preparation of sub-200 nm poly(lactide-co-glycolide) microspheres for site-specific drug delivery. *J. Control. Rel.* 25, 145-153.
- Gan, C. and Feng, S. 2010. Transferrin-conjugated nanoparticles of Poly(lactide)-d- α -Tocopheryl polyethylene glycol succinate diblock copolymer for targeted drug delivery across the blood-brain barrier. *Biomaterials.* 31(30), 7748-775.
- Soni, V., Kohli, D.V., Jain S.K. 2008. Transferrin coupled liposomes as drug delivery carriers for brain targeting of 5-florouracil. *J. Drug Target.* 13, 4, 245-250.
- Vanderhoff J. W., El Aasser M. S., Ugelstad J. 1979. Polymer emulsification process. US Patent 4,177,177.
- Vasir, J.K., and Labhasetwar, V. 2007. Biodegradable nanoparticles for cytosolic delivery of therapeutics. *Adv. Drug Del. Rev.* 59, 718-728.